Nuclear Medicine Imaging in Cancer

Masha Maharaj
Department of Nuclear Medicine
University of Limpopo, Polokwane Campus, South Africa

Nisaar Korowlay
Division of Nuclear Medicine
Tygerberg Hospital, Stellenbosch University, South Africa

1 Introduction

The basic pathological unit in cancer is a colony of cells over which there is a loss of normal regulatory mechanisms. At a functional level this results in uncontrollable proliferation of an abnormal cell line driven by oncogenic signals, impaired differentiation, and invasion of other tissues leading to metastases. It has become increasingly obvious that the changes of a cancer observed on a molecular level bear increment value toward the outcome of therapy. In 2011, Hanahan and Weinberg (Hanahan & Weinberg 2011) described six biological hallmarks of cancer acquired during the multistep development of human tumours. The hallmarks constitute an organizing principle for rationalizing the complexities of neoplastic disease; sustaining proliferative signalling, evading growth suppressors, resisting programmed cell death (apoptosis), limitless replicative potential, sustained angiogenesis, tissue invasion and metastasis, changes in metabolism and tumour promoting inflammatory alterations and interactions (Multhoff & Radons, 2012; Marnett, 2012). The improved knowledge of tumour-specific and tumour-associated processes have motivated and resulted in the development of new tools for diagnosis (imaging) and targeted therapy in Nuclear Medicine (Jaffer & Weissleder, 2005; Beirsack *et al*., 1992; Haberkorn *et al*., 2011; Debergh *et al*., 2012; Weisleder, 2006; Ray, 2011; Sullivan & Gatsonis, 2011; Valotassiou *et al*., 2012).

The aim of this chapter is to assist the student and clinician in sufficient understanding of Nuclear Medicine pertinent to areas of imaging of cancer. The introduction briefly provides insight into the tracer and equipment in Nuclear Medicine. The radiopharmaceuticals have been discussed in parallel with the biological hallmarks of cancer; metabolic, proliferation, angiogenesis, hypoxia and apoptosis. Included in the chapter is summary of existing SPECT (single photon emission computer tomography) radiopharmaceuticals which have also made their mark in general imaging in cancer and cancer management. A brief introduction into Theranostics is provided at the end.

1.1 The Tracer Principle:

The tracer principle, founded by Nobel Hevesy G in 1912 (Leitha, 2009), suggested that radioactive elements had identical chemical properties to the nonradioactive form and therefore could be used to trace chemical behaviour in solutions or in the body. The basis of Nuclear Medicine involves the administration of small amounts of radiopharmaceuticals (radiolabelled tracer) that emit radiations such as gamma (γ)-rays, x-rays, beta (β)-particles, alpha (α)-particles or positrons. The administration of small amounts of the relevant tracer allows one to directly observe the physiological process under study, without disturbing that process under investigation. Imaging of the radiotracers allows for monitoring biological processes non-invasively. The administration of low dose radiopharmaceuticals exposes the patient to low levels of ionizing radiation which is consistent with ALARA (As Low As Reasonably Achievable). Avoiding harmful consequences of radiation of which carcinogenesis is a primary concern (Fahey, 2011).

1.2 Equipment

1.2.1 Single Photon Emission Computer Tomography (SPECT)

The Gamma camera, also called a Scintillation camera or Anger camera has been developed since 1944. It is a device used to use in Nuclear Medicine to image γ-radiation emitting radioisotopes (Table 1) to view and analyse images of the human body or the distribution of medically injected, inhaled, or ingested radionuclides emitting gamma rays, producing a two dimensional (2D) image, a technique known as scintigraphy. SPECT is a scintigraphic technique in which a computer-generated image of local radioactive

tracer distribution in tissues is produced through the detection of single-photon emissions from radionuclides introduced into the body that is able to provide true three-dimensional (3D) information. This information is typically presented as cross-sectional slices through the patient, but can be freely reformatted or manipulated as required. SPECT camera may be combined with a computerised tomography (CT) unit to form a hybrid system and fusion imaging of the physiology and anatomy of the area/s being scanned. Combined SPECT/CT devices provide both the functional information from SPECT and the anatomic information from CT in a single examination. SPECT/CT acquisitions can include the whole body, a limited portion of the body, or an organ. The method of attenuation correction is the use of CT transmission data with SPECT/CT scanners (Mariani *et al*., 2008).

Nuclide	Half-life	Decay	Major emissions kilo electron volt (keV)
Technetium-99m (99mTc)	6 hours	Isomeric transition (I.T).	140
Gallium-67 (67Ga)	78 hours	Electron Capture (E.C.)	93, 184, 296, 388
Indium-111 (111In)	67 hours	E.C.	172, 247
Iodine-123 (123I)	13 hours	E.C.	159
Iodine-125 (125I)	60 days	E.C.	27
Iodine- 131 (131I)	8 days	Beta emission(β-)	364
Thallium-201 (201Tl)	73 hours	E.C.	Hg daughter X-ray emission 69-81

Table 1: Selected radionuclides for SPECT imaging.

1.2.2. Positron Emission Tomography (PET)

PET has been in existence since the 1970s and has developed from a research technique to a current state-of-the-art clinical imaging tool. Through positron-emitting radionuclide labelling, PET allows in-vivo imaging of physiologically and pathologically important molecules containing basic organic chemical elements such as carbon, fluoride, oxygen and nitrogen. The molecular and/or metabolic information provides essential contribution to the diagnosis, evaluation and prognosis of disease. This has impacted on effective patient management.

PET radionuclides emit positrons (β^+) particles (positively charged electrons). The most commonly used radionuclide, fluorine-^{18} (^{18}F), has a median range of only 0.2 mm in tissue and a maximum range of 2.4 mm. At the end of its trajectory, the positron interacts with an electron in a nearby atom and both are annihilated resulting in the emission of two gamma (γ) photons, each with energy of 511 keV. These photons move away from the point of annihilation in opposite directions at almost 180° straight line.

PET is a volumetric technique optimized for detection of these annihilation photons. It allows precise tracking of the spatial and temporal distribution of positron emitting radiopharmaceuticals in patients and represents a unique functional tomographic imaging modality based on the biochemical handling of chemicals by tissues of the body (Zeigler, 2005; Schyler, 2004; Chen & Chen, 2011).

The two instrumental PET radionuclides currently in clinical use include ^{18}F and ^{68}Ga. ^{18}F is cyclotron produced with a physical half-life of 110 minutes. The development of the radiopharmaceutical ^{18}F-fluorodeoxyglucose (^{18}F-FDG), a glucose analogue taken up avidly by the majority of malignant tumours, has resulted in it being used routinely in the management of many cancer patients.

^{68}Ga has a physical half-life of 68 min. Its parent, Germanium- 68 (^{68}Ge) is accelerator produced on Ga_2O_3 targets with a half-life of 270.8 days and decays by electron capture. The major advantage of

^{68}Ga over ^{18}F is its production from an in-house generator, making ^{68}Ga supply independent of a nearby cyclotron. ^{68}Ge/^{68}Ga generator systems have been developed since the late 70's, however, their relevant clinical use and further use in development of PET radiopharmaceuticals has been launched recently (Khan *et al*., 2009; Maecke *et al*., 2005). Table 2 illustrates a summary of current regulatory status of PET tracers.

The last 15 years have seen an exponential growth of PET, and even more since the introduction of hybrid positron emission tomography/computed tomography (PET/CT). The term 'one-stop-shop' has been dubbed to indicate the proficiency of obtaining physiological and anatomical information in a single investigation. The advantages of combining PET and CT include its superior lesion localisation in accurate anatomical/functional registration; a better distinction between physiological uptake and pathological uptake; consolidation of functional and anatomical imaging; and a benefit in shorter total scan time enhancing patient comfort and minimizing issues with claustrophobia and movement.

Mechanism	Tracer	*PET (regulatory status)
Glucose metabolism	Glucose analogue	Food and Drug Administration (FDA) approved
Lipid and Fatty Acid metabolism	Choline Acetate	Investigational/ Institutional Clinical use
DNA metabolism	Thymidine analogues	Investigational/ Institutional Clinical use
Amino Acids and Protein metabolism	Dopamine Tumour specific Receptors Tumour targeting Antibodies Guanidine analogue Gene expression	Investigational/ Institutional Clinical use
Angiogenesis	Vacular endothelial growth factor and receptors Integrins Matrix metalloproteinases Other angiogenesis targets	Investigational/ Institutional Clinical use
Iodine metabolism	Iodine	Investigational/ Institutional Clinical use
Hypoxia	Nitromidazole derivatives	Investigational/ Institutional Clinical use
Apoptosis	Annexin-V	Investigational/ Institutional Clinical use

Table 2: Summary of PET tracers with current regulatory status (Hicks & Hofman, 2012).

2 Radiopharmaceuticals

Table 3 shows an overview of radiopharmaceuticals that will be discussed in this section.

2.1. Metabolic

2.1.1. Glucose metabolism

^{18}F-Fluorodeoxyglucose (^{18}F-FDG)

^{18}F -FDG provides information about the rate of glucose metabolism in the body. ^{18}F has a physical half-life of 110 minutes and suitable kinetics for imaging with optimal resolution (Gunn *et al*., 2002). Malignant cells show increased glucose uptake in vitro and in vivo, and this process is thought to be mediated by glucose transporters. There are estimated 14 known glucose trans-porter (GLUT) protein subtypes,

Metabolic	Glucose metabolism	FDG
	Lipid and fat	Choline
		Acetate
	Proliferation (DNA metabolism)	Thymidine analogues
	Amino Acids and Protein metabolism	Radiolabelled amino Acids
		Radiolabelled peptides
		Somatostatin Receptor analogues
		Dopamine
		Tumour specific Receptors
		Monoclonal Antibodies
		Guanidine analogue (Metaiodobenzylguanidine)
		Gene expression
	Iodine metabolism	Iodine
Angiogenesis		Vacular endothelial growth factor and receptors Integrins Matrix metalloproteinases Other angiogenesis imaging targets
Hypoxia		Nitromidazole derivatives
Apoptosis		Annexin-V
General tumour imaging radiopharmaceuticals	Skeletal	Methylene Diphosphonate
		Flouride
	Mitochondrial activity	Methoxy-isobutyl-isonitrile
	Transferrin receptor mechanism	Gallium 67 citrate
	Na-K adenosine-tri-phosphatase (ATP) system	Thallium 201
	Lipophilic brain perfusion agent converted by glutathione	Hexamethyl propylamine oxime (HMPAO)
General use of Nuclear Medicine in management and monitoring in Cancer	Equilibrium-gated Radionuclide Angiocardiography	Red blood cells
	Sentinel Node Imaging	Colloid particles

Table 3: Overview of Radiopharmaceuticals discussed in Section 2

with Glut1 and Glut3 expressed to a greater degree in a variety of carcinomas. This up-regulation of Glut protein enhances tumour glucose metabolism (Kyoichi *et al*., 2011). ^{18}F -FDG is transported into tumour cell and processed the same physiological way as glucose is processed. After phosphorylation to ^{18}F -FDG-6-phosphate by hexokinase, ^{18}F-FDG-6-phosphate cannot be metabolized further in the glycolytic pathway and becomes trapped in the cell because of its negative charge. In a normal cell this process is reversed by glucose-6-phosphatase. In most tumour cells there is overexpression of Hexokinase and down-regulation of glucose-6-phosphatase which results in the accumulation of ^{18}F-FDG-6-phosphate in the cell (Kyoichi *et al*., 2001).

The assessment of uptake of FDG is subjective (visually) and objectively, using an FDG uptake index with Standard uptake values (SUV). The SUV method takes into account the injected dose of FDG as well as the patient's body mass and is calculated as: (counts within region of interest)/ (body weight x dose injected). Studies have demonstrated that SUVs may vary considerably depending on the clinical scenario; inflammation, size of lesion under 1 cm in size may be underestimated and benign lesions may

express high SUV's. SUV is also subjective to other sources of variability which are not controlled such as glucose level, length of the uptake period, body weight, body composition, recovery coefficient and partial volume effect (PVE), image parameters and image protocols (Wiyaporn *et al*., 2010). The pivotal role of the SUV would be in the follow-up of the patient in monitoring response to therapy (Joseph, 2004).

Gambhir *et al*., 2001, from a collection of 419 articles from 1993 to 2000 estimated the average ^{18}F-FDG PET sensitivity and specificity across all indications in oncology at 84% (based on 18,402 patient studies) and 88% (based on 14,264 patient studies), respectively (Tinsu & Osama, 2008).

The European Association of Nuclear Medicine (EANM), British Nuclear Medicine Society (BNMS) and Society of Nuclear Medicine (SNM) guidelines have illustrated the current clinical indications of FDG-PET (SNM Procedure guidelines; BNMS Procedure guidelines; EANM Procedure guidelines). Assessment at primary presentation in the diagnosis of unknown primary malignancy, differentiation of benign and malignant lesions (such as a solitary lung nodule, especially in case of discrepant clinical and radiological estimates of the likelihood of cancer). Staging on presentation in non-small-cell lung cancer, T3 oesophageal cancer, Hodgkin's disease, non-Hodgkin's lymphoma, locally advanced cervical cancer, ENT tumours with risk factors and locally advanced breast cancer (Karaosmanoğlu & Blake, 2012). Evaluation of response to therapy in malignant lymphoma and GIST (Zanoni etal, 2011; Park *et al*., 2011). Restaging in the event of potentially curable relapse for FDG avid tumours. Establishing and localizing disease sites as a cause for elevated serum markers (this includes colorectal, thyroid, ovarian, cervix, melanoma, breast and germ-cell tumours). Image guided biopsy and use in radiotherapy planning have made a colossal impact (Arens & Troost, 2011).

Variable physiological FDG Uptake is seen in normal structures brain, the nasal turbinates', pterygoid muscles, extraocular muscles, brown fat, vocal cord uptake, thyroid, parotid, submandibular glands, and lymphoid tissue of the adenoids, upper Waldeyers ring, brain, heart, kidneys and urinary tract. There is some degree of FDG accumulation in the muscular system, and is increased by exercise. Gastrointestinal tract uptake varies from patient to patient. Physiological thymic uptake may be present in children, in young adults and in patients with regenerating haemopoietic tissues.

False-positive findings include inflammation, infection, granulomatous processes and benign neoplasms. False negative results may arise from low FDG avidity tumours. These vary from well differentiated tumours such a prostate cancer and neuroendocrine tumours to metastatic lesions from FDG avid primaries such as sarcomas. Lack of uptake may arise from relatively low glucose metabolism, high mucin content, low proliferation rates and necrosis (Freeman& Blaufox, 2013). A modulatory factor for ^{18}F-FDG uptake has been associated with the overexpression of P-glycoprotein in tumours, the exact underlying mechanism and relationship to glucose metabolism remains unknown. Overexpression of P-glycoprotein is an in vivo marker of multidrug resistance (Satoru *et al*., 2009). In vitro studies using cancer cell lines, the uptake of ^{18}F-FDG was markedly decreased by the inhibition of Glut1 or hypoxic inducible factor-1alpha (HIF-1α), whereas, Glut1 up-regulation by the induction of HIF-1α increased the ^{18}F-FDG uptake, indicating that cellular uptake of ^{18}F-FDG is mediated by Glut1 and that the expression of Glut1 protein was regulated by HIF-1α. (Kyoichi *et al*., 2010). Although the mechanism is not fully understood, FDG negative soft tissue metastases of FDG avid primary sarcomas have been reported (Roberge *et al*., 2012).

Interpretation of structures/lesions adjacent, within or in proximity to an anatomic structure with inherently high FDG uptake such as the brain or tonsils may make it difficult to distinguish pathologic from physiologic metabolic activity.

Interpretation may be limited by artefacts generated by CT-based attenuation correction. Metallic devices can demonstrate falsely elevated FDG uptake. Intravenous contrast material is present in venous structures during CT but not during the PET portion of the examination causing areas of linear artefact (mimicking intense FDG accumulation) on the attenuation-corrected PET. Respiration artefacts and motion artefacts are common. Truncation may cause artefacts due to differences in size of field of view (FOV) CT (50 cm) and PET (70 cm).

Preparation may vary in relation to the area being investigated as per centre protocol. Generally the patient should be kept warm to limit brown fat activity. They should be comfortable during uptake and scan. They should keep quiet at least 30 min prior to and after the injection. The protocol may require a head holder or frame. The patient should fast 6 hours prior to study. The random glucose level <7 mmol/l (or <120 mg/dl). All fertile females should have a pregnancy test prior to injection. It should be recorded when the last chemotherapy was done and usually at least 10 days is acceptable to perform the study. The study may be performed at least 3 months post radiation therapy and surgery. The patient must be able to lie still for 20-45 minutes. The average radiation dosimetry for 350MBq is 7mSv for PET and 3-5mSv for the low dose CT component. (Poeppel *et al*., 2009)

2.1.2. Lipid and Fatty Acid Metabolism

Choline

All cells in the body absolutely require choline. Choline is needed for the synthesis of phospholipids in cell membranes, methyl metabolism, cholinergic neurotransmission, transmembrane signalling, and lipid-cholesterol transport and metabolism. The uptake mechanism of choline and fluorocholine in tumour cells is of great interest. The backbones of cell membranes are made of phospholipid bilayers, of which the major component is phosphatidylcholine. The cell membranes are duplicated at the same rate as the rate of cell duplication.

Choline is a precursor for the synthesis of the neurotransmitter, acetylcholine. In the cell, choline can be phosphorylated, acetylated or oxidized. On a basic molecular level, phosphorylcholine is converted into phosphatidylcholine (lecithin) which is then incorporated into membrane synthesis. The phosphorylation of choline is catalysed by the enzyme choline kinase which has been implicated in malignant transformation of cells associated with the induction of choline kinase activity resulting in increased levels of phosphorylcholine. There is an increased demand of choline and phosphorylcholine incorporated into tumour cells in order to match the rapid rate of cell turnover.

In 1997, ^{11}C Choline was introduced as a potential PET tracer to image brain and prostate cancer. The inconvenient short half-life of ^{11}C and the rapid oxidization of ^{11}C-choline in vivo encouraged the development of ^{18}F-labeled choline analogues (FCH) and ^{18}F-fluoroethylcholine (FECH). These radiotracers were found to be good substrates for the enzyme choline kinase, but not for the enzymes involved in the oxidation of choline. The uptake of radiolabeled choline and fluorocholine represents exactly the duplication rate of tumour cells, and radiolabeled compounds present as extremely useful tools in the molecular evaluation of cancer.

Studies in prostate cancer have shown using and comparing FCH and FDG, more lesions were identifiable with FCH, including lesions of the prostate, bone, and soft tissue. Oncological applications have included evaluating high grade gliomas, anaplastic astrocytomas and primary hepatocellular cancer (but have low affinity for metastatic lesions to liver from colorectal cancer). (Picchio & Castelluci, 2012; Jadvar, 2011).

Acetate

Acetate is taken up by cells and activated to acetyl-CoA in both the cytosol and mitochondria by acetyl-CoA synthetase. Acetyl-CoA is a common metabolic intermediate for synthesis of cholesterol and fatty acids, which are then incorporated into the membrane. In normal cells and in myocardium, Acetyl-CoA is oxidized in mitochondria to carbon dioxide and water. In tumour cells, acetate is converted into fatty acids by fatty acid synthetase (overexpressed enzyme in cancer cells).

Prostate cancer is the most prevalent tumour for which imaging by PET with ^{18}F-FDG has been found to be generally unsatisfactory (Jadvar, 2011). The 60%–70% sensitivity of ^{18}F-FDG PET for prostate cancer is not high enough to justify its routine clinical use for staging or restaging of this disease. The poor performance of ^{18}F-FDG PET is likely related to the low glucose metabolic rate that results from the relatively slow growth of most prostate cancers as well as to other factors, including significant excretion of ^{18}F-FDG into the adjacent urinary bladder, making detection of tumour uptake difficult. PET with ^{11}C-Acetate (^{11}C-ACE) has a high sensitivity for detection of prostate cancer and several other cancers that are poorly detected with ^{18}F-FDG. The short half-life of ^{11}C limits its general availability. ^{18}F-Fluoroacetate (^{18}F-FAC) is an analogue of acetate with a longer radioactive half-life. Results indicate that ^{18}F-FAC is retained longer in tumour tissue than in other organs, suggesting that it is a useful tracer for PET tumour imaging. The liver and kidney appear to be the major metabolic organs. It has not yet been determined as to the precise mechanism for the incorporation of ^{18}F-FAC into tumours. Several authors have indicated ^{18}F-FAC is a useful alternative to ^{11}C-ACE for the detection of prostate tumours. Future indications may include other neoplasms with relatively low glucose use.(Ponde *et al*., 2007).

2.1.3. Proliferation (DNA metabolism)

Thymidine Analogues

Increased cellular proliferation, increased mitotic rate, cell proliferation, and lack of differentiation were regarded as the main factors responsible for accelerated growth of malignant tissue. In the 1950s, ^{3}H-Thymidine was introduced to measure thymidine incorporation into DNA (thymidine labelling index) in tumour tissue. ^{11}C-thymidine was prepared but was not optimal for routine imaging studies due to the short half-life and the rapid catabolism of thymidine after injection. These limitations led to the development of analogues that are resistant to degradation and can be labelled with radionuclides more conducive to routine clinical use, such as ^{18}F (Kumar, 2008).

Thymidine analogues that have been studied the most are 39-deoxy-39-fluorothymidine (FLT) and 1-(29-deoxy-29-fluoro-1-b-D-arabinofuranosyl)-thymine (FMAU). Both are resistant to degradation and track the DNA synthesis pathway. FLT enters tumour cells both via a nucleoside transporter and partly via passive diffusion. Inside proliferating cells, FLT is accepted as a substrate by thymidine kinase 1 (TK-1), which phosphorylates it, thereby trapping it in cells. FLT-monophosphate is further phosphorylated to di- and triphosphate forms. FLT-triphosphate is not significantly incorporated into DNA, unlike other thymidine analogues. The majority of FLT persists as mono- and triphosphates in the cytosol (Shankar, 2007). Due to dephosphorylation of FLT-monophosphate by the enzyme deoxynucleotidase, some FLT is effluxed from cells, but at a slower rate, providing a significant period of relatively stable tracer retention for imaging (Bading & Shields, 2008).

The entrapment of the radiotracer within the cell and allows noninvasively measuring cellular proliferation in vivo in malignant tumours and organ tissues. It is incorporated by the normal proliferating marrow and is glucuronidated in the liver. FMAU can be incorporated into DNA after phosphorylation

but shows less marrow uptake. It shows high uptake in the normal heart, kidneys, and liver, in part because of the role of mitochondrial thymidine kinase-2. Early clinical data for ^{18}F-FLT demonstrated that its uptake correlates well with in vitro measures of proliferation. Although ^{18}FFLT can be used to detect tumours, its tumour-to-normal tissue contrast is generally lower than that of ^{18}F-FDG in most cancers outside the brain. The most promising use for thymidine and its analogues is in monitoring tumour treatment response, as demonstrated in animal studies and pilot human trials. Further work is needed to determine the optimal tracer(s) and timing of imaging after treatment. Oncological applications thus far of Thymidine include primary lung cancer with recorded sensitivity of 72% and specificity of 89% (Yap *et al*., 2006), brain malignancies mostly high grade gliomas iii/iv, lymphoma demonstrating high uptake in aggressive type cell, breast cancer for early assessment of response to chemotherapy within 2 weeks of therapy, colorectal cancer although it has not been found to be useful for liver metastasis, it was found useful in oesophageal cancer by van Westreenen, in head and neck cancer uptake correlates with the aggressiveness of the tumour, in melanoma and soft tissue sarcoma of the extremities (Plotnik *et al*., 2010).

Treatment with chemotherapy and radiation has been shown to reduce FLT uptake in these cancer models.

FLT-PET should not be regarded as an overall staging tool for cancer. There is lower overall uptake of FLT in tumours and higher background activity in the liver and bone marrow. It is not expected to have the same outstanding sensitivity as FDG-PET for tumour detection. FLT-PET should be considered a powerful addition to staging by FDG-PET. Providing additional diagnostic specificity for proliferating tissues and important biological information that could have implications in treatment selection or monitoring (Salskov *et al*., 2007).

2.1.4. Amino Acids and Protein Metabolism

Amino Acids (AAs) are precursors for many biomolecules, such as hormones or neurotransmitters, such as the DNA or RNA precursors adenine and cytosine, sphingosine (derived from serine), histamine (derived from histidine), thyroxine, adrenaline and melanine (all derived from tyrosine), and serotonin (derived from tryptophan). In addition to being metabolic precursors, amino acids can be crucial in metabolic cycles as they enter several metabolic cycles and undergo metabolism, transamination and decarboxylation. AAs may enter the cell by simple diffusion or are transported via more than 20 membrane transport systems. AAs may also originate within the cell being derived from intracellular protein recycling.

Proteins play crucial roles in virtually all biological processes. Nearly all chemical reactions in biological systems are catalysed by enzymes, and nearly all enzymes are proteins. Many small molecules are transported and stored through specific proteins. Proteins are the major component of muscle. They are important in mechanical support (collagen), in immune protection (antibodies), nerve impulse transmission (receptors) and in control of growth and differentiation (growth factors, DNA control proteins and others). A protein is built from a set of 20 amino acids. It is characterized by an amino- and a carboxyl-group and twenty side-chains, varying in size, shape, charge, hydrogen-bonding capacity and chemical reactivity. Polypeptide chains (proteins) are formed by linking amino acids through peptide bonds. The rate of protein synthesis depends on processes that are subject to complex regulations. Genes specify the unique amino acid sequence of proteins. Cells regulate which specific proteins are synthesized and also the total amount of protein synthesis. (Kanwar *et al*., 2011; Mankoff *et al*., 2008; Badgaiyan, 2011; Nil *et al*., 2011).

Radiolabelled Amino Acids

Malignant transformation increases the use of amino acids for energy, protein synthesis, and cell division. Tumour cells often over-express transporter systems resulting in an overall increase in AA transport and /or an increase in protein synthesis rate by tumour cells. Carboxyl-^{11}C-L-leucine, ^{11}C-L-methionine, and ^{11}C-L-tyrosine were introduced as tumour-imaging agents for the estimation of protein synthesis approximately 30 years ago. ^{18}F-labeled tracers developed are based on tyrosine and phenylalanine AAs. The tumour uptake of the ^{18}F-labeled AAs is related to carrier-mediated active transport, and not to protein synthesis. **^{11}**C-methionine is an amino-acid analogue. It has been found useful in low-grade glioblastoma, glioblastoma (mild uptake), and meningioma (high uptake). More recently, artificial amino acids such as L-3-^{123}I-iodo-alpha-methyl-tyrosine (IMT) or L-3-^{18}F-fluoro-alpha-methyl-tyrosine (FMT), O-2-^{18}F-fluoroethyl-L-tyrosine (FET), ^{18}F-fluoro-L-phenylalanine, ^{18}F-fluoro-L-proline and ^{11}C-methyl- alpha-aminoisobutyric acid have been studied.

Radiolabelled Peptides

Peptides have many key properties including fast clearance, rapid tissue penetration, and low antigenicity, and can be produced easily and inexpensively. However, there may be problems with in vivo catabolism, unwanted physiologic effects, and chelate attachment.

Somatostatin Receptor Analogues

The Somatostatin receptor (SSR) analogues have made their greatest impact in the management of neuroendocrine malignancies. The hypothalamus, adrenals and the pancreas produce somatostatin, a cyclic tetradecapeptide (SST-14) and the congener SST-28. Somatostatin modulates neurotransmission in the central nervous system (as a neurotransmitter) and regulates the release of growth hormones and thyrotropin (as a neurohormone). It also has a regulatory role in the gastrointestinal tract, as well as in the exocrine and endocrine pancreas. The actions of SST are mediated through specific membrane receptors. These receptors are expressed in various organs and tissues such as the pituitary, the pancreas and cells of the immune system. To date five subtypes of human somatostatin receptors (SSTR1-5) have been cloned and characterized. The expression of high-affinity and -density SSTRs by certain class of neuroendocrine cancers made it attractive to use radionuclide-imaging techniques to detect, stage and diagnose these cancers and their distal metastases. SSTR are also expressed in renal cell carcinoma, small cell lung cancer, breast cancer, prostate cancer and malignant lymphoma.

^{123}I-Tyr3-octreotide was the first radiopeptide SSTR tracer for which proof of principle was obtained. ^{111}In-DTPA-(D)Phe-1-octreotide is the commercially available radiopeptide SSTR tracer of choice for the detection and follow-up of neuroendocrine tumours (OctreoScan®, Tyco). It can be conveniently prepared using a kit. ^{111}In-DOTA-lanreotide is synthesized using the commercially available lanreotide (Somatuline ®) and 1,4,7,10-tetraazacyclo-dodecane-N,N′,N′′,N′′′-tetraacetic acid (DOTA) as starting materials. It is the most successful radiopeptide for tumour imaging. The use of OctreoScan as such analogue is being replaced with new peptides such as DOTATATE (DOTA-D-Phe^{1}-Tyr^{3}-Thr^{8}-octreotide) and DOTATOC (DOTA-Phe^{1}-Tyr^{3}-octreotide).

^{99m}Tc-depreotide (NeoTect) is an SSTR receptor based radiopharmaceutical which, in contrast to octreotide based ligands, also binds to SSTR3 with high affinity. It is available from GE-Amersham in Europe and Schering in the USA. (NeoTect). It has a high sensitivity and specificity for lung cancer lesion detection.

^{68}Ga is available from an in-house generator rendering ^{68}Ga radiopharmacy independent of an on-site cyclotron. ^{68}Ga has a half-life of 68 min and decays by 89% through positron emission. The parent, ^{68}Ge, is accelerator produced and decays with a half-life of 270.8 d by electron capture. Radiopeptides for ^{68}Ga labelling have been developed and tested preclinically for the targeting of somatostatin receptors, the melanocortin-1 receptor, and the bombesin receptor. The most valuable role of ^{68}Ga PET is in SSTR imaging. ^{68}Ga-DOTATOC and ^{68}Ga-DOTANOC (^{68}Ga-[DOTA]-1-Nal^{3}-octreotide) are the most prominent radiopharmaceuticals used currently. Clinical studies demonstrated higher sensitivity localizing neuroendocrine tumours with ^{68}Ga-DOTATOC compared to ^{111}In-Octreotide, ^{111}In-DTPA Octreotide and ^{18}F-FDG. The 2010 EANM 'Procedural guideline for PET/CT Tumour Imaging with ^{68}Ga-DOTA conjugated peptides: ^{68}Ga-DOTA-TOC, ^{68}Ga-DOTA-NOC, ^{68}Ga-DOTA-TATE,' stated the primary indication of ^{68}Ga-DOTA-conjugate peptides PET/CT is the imaging of NETs, which usually express high density of SST receptors. Less frequently it can be used in non-NET imaging, particularly if treatment with radiolabeled therapeutic SST analogues is considered. Currently available PET tracers are ^{68}Ga and ^{18}F somatostatin analogues and ^{64}Cu TETA-Octreotide. Oncological applications include identifying/localizing neuroendocrine tumours, evaluating disease extent, monitoring effects of therapy, selecting patients for therapy, prognostic indicator.(Laverman *et al*., 2012; Gnanasegaran *et al*., 2005; Baum *et al*., 2008; Baum *et al*., 2005; Rufini *et al*., 2006).

Radiolabelled peptide therapy is usually indicated for patients with widespread disease that is not amenable to focused radiation therapy or is refractory to chemotherapy. Radiolabelled peptides such as ^{111}In-pentetreotide, ^{90}Y-DOTA-Phe1-Tyr3-octreotide, ^{90}Y-DOTA-lanreotide, and ^{177}Lu-DOTA-octreotate are indicated for the treatment of patients with neuroendocrine malignancy. (Kam *et al*., 2012; Turaga &kvols, 2011).

Dopamine

Neuroendocrine tumours (NETs, APUDomas) can be small and situated almost throughout the body. This heterogeneous group of tumours take up amino acids, transform them into biogenic amines (dopamine and serotonin) by decarboxylation, and store the amines in vesicles; this is the so-called APUD (amino precursor uptake and decarboxylation) concept. L-Dihydroxyphenylalanine (L-DOPA) is a precursor of catecholamine's (dopamine, noradrenalin and adrenalin). Its conversion to dopamine is catalysed by the aromatic amino acid decarboxylase (AADC). Pancreatic islet cells take up L-DOPA where AADC converts it to dopamine. Ahlström *et al*. (1995) were the first to visualize pancreatic NETs with ^{11}C–L-dihydroxyphenylalanine (^{11}C-LDOPA) PET, and the same group in 1996 also demonstrated that the in vivo uptake was due to decarboxylation.

3,4-dihydroxy-6-^{18}F-fluoro-L-phenylalanine (^{18}F-FDOPA) was developed to examine the transport of dopamine precursor from the plasma (Seibyl *et al*., 2007). FDOPA in oncology has been proposed to evaluate melanomas, neuroendocrine tumours, medullary thyroid carcinoma, pheocromocytomas, gastrointesitinal carcinoid tumours, brain tumours; mostly metastatic tumours and malignant gliomas superior in evaluating recurrent low-grade and high-grade gliomas. Tumor uptake of ^{18}F-FDOPA has been reported to be similar to that of 11C-methionine. ^{18}F-FDOPA accumulation is very high in the kidneys and urinary bladder which may be a problem in studying the tail of the pancreas (Fouge *et al*., 2011).

Jora, *et al*., did a comparative evaluation of ^{18}F-FDOPA, ^{13}N-AMMONIA, ^{18}F-FDG PET/CT and MRI in primary brain tumours and found ^{18}F-FDG uptake correlated with tumor grade (Jora *et al*., 2011). Although ^{18}F-FDOPA PET could not distinguish between tumor grades, it is more reliable than ^{18}F-FDG and ^{13}N-Ammonia PET for evaluating brain tumors. ^{18}F-FDOPA PET may prove to be superior to MRI in

evaluating recurrence and residual tumor tissue. ^{13}N-Ammonia PET did not show any encouraging results (Oikonen, 2005).

Tumour Specific Receptors

Tumour receptors have been some of the earliest targets for cancer therapy, with notable successes in the treatment of endocrine-related cancers such as breast, prostate, and thyroid cancers. Advances in molecular cancer biology have revealed an ever-increasing number of tumour targets, many of which are receptors, such as the epidermal growth factor (EGF) receptor (EGFR). The ability to measure the expression of tumour receptors is essential for selecting patients for receptor-targeted therapy. Tumour receptor imaging emphasizes important emerging themes in molecular imaging: characterizing tumour biology, identifying therapeutic targets, and delineating the pharmacodynamics of targeted cancer therapy. The advantages of imaging include non-invasiveness, the ability to measure receptor expression for the entire disease burden and thereby to avoid the sampling error that can occur with heterogeneous receptor expression, and the potential for serial studies of the in vivo effects of a drug on the target. The estrogen receptor (ER) system is an illustrative example of a receptor system with relevance to cancer. (Mankoff *et al*., 2008).

Flourine-^{18}-flouro-17-β-estradiol (FES)

Estradiol is the most potent form of estrogen in the body and binds to ERs. It is found in the cell nucleus of the female reproductive tract, breast, pituitary, hypothalamus, bone, liver, and also in various tissues in men. Estradiol is a naturally occurring agonist ligand for the ER. The molecular mechanism of estradiol action through the ER has been well studied. Estradiol is lipophilic, allowing access across cell membranes to the ER, a nuclear receptor. The ER has 2 receptor subtypes: ER-a and ER-b. ER-a serves mainly as an activator of downstream events related to breast and female sex organ function. The function of ER-b is less well understood; in some situations, ER-b may inhibit ER-a by forming a heterodimer with ER-a. Estradiol binding to ER-a in the nucleus results in dimerization of the receptor and allows interactions with specific DNA sequences known as the estrogen response elements, leading to the selective regulation of target gene transcription.

ER activation leads to different physiologic actions in different tissues. The ER Status: the growth of breast epithelial cells depends on estrogen acting through an ER and the induction of progesterone receptor. The ER status is an important prognostic factor in breast cancer. ER tumours have a slower rate of growth and a better response to hormonal therapy.

Despite the importance of tumour receptors in carcinogenesis and tumour growth, tumour receptors are not always effective targets for cancer treatment, because some cancers can sustain growth independently of receptor activation. In some situations, growth independence is accompanied by a loss of or a reduction in receptor expression, such as in ER negative (ER-) breast cancers. In such situations, the absence of receptor expression indicates a negligible chance of success of receptor-targeted therapy. In other situations, even though a receptor is still present, receptor pathway activation is not required for growth. In 30 to 40% of all breast cancers there is no estrogen receptors expression (ER-). Although 70% of breast cancers express the ER, only 50%–75% of ER-expressing primary breast cancers respond to endocrine therapy, and even fewer recurrent tumours respond. A non-invasive method to evaluate and quantify the presence of ER on the tumour and its metastases would better select patients for treatment, and predict the therapeutic response. The radiolabeled estrogen analogue identified is 16-^{18}F-fluoro-17-estradiol (FES) and has shown the most promise in quantifying the functional ER status of breast cancer,

both in the primary tumour and in metastatic sites. ^{18}F-flourotamoxifen is still being investigated (Mankoff *et al*., 2008).

Flourine ^{18}-Flouro- dihydrotestosterone

Androgen receptors play an important role in growth and proliferation of prostate cancer. The androgen status is a prognostic indicator. Dihydrotestosterone is the primary ligand for androgen receptors. Anti-androgen is one of the most effective treatments in the management of prostate cancer. Flourine-18-flouro-dihydrotestosterone (FDHT) is useful in monitoring treatment response. Androgen resistance of the lesion is shown by a negative FDHT scan and positive FDG scan. (Mankoff *et al*., 2008).

Radioimmunoscintigraphy

Radioimmunodetection or radioimmunoscintigraphy uses tumour targeting antibodies or antibody fragments, labelled with a radionuclide suitable for external imaging, for the detection of specific cancers. Monoclonal antibodies have been developed against a variety of antigens associated with tumours and have been shown to target tumours with minimal side effects. Numerous radionuclides suitable for external imaging have been conjugated to antibodies, or antibody fragments, and the radioimmuno-conjugates have been shown to be stable in vivo. Several factors have accelerated the expansion of the role of antibodies in cancer imaging. It is the identification of cell surface biomarkers as imaging targets coupled with advances in antibody technology, which facilitate the generation of antibodies optimized for non-invasive imaging.

Radioimmunoscintigraphy has been shown to be of benefit in the detection of occult disease, in the management of patients with potentially resectable disease, and for the evaluation of lesion recurrence and therapeutic response. Radiolabelled antibody imaging in prostate cancer has been shown to be useful in risk stratification and in patient selection for loco-regional therapy. Antibody imaging can provide a sensitive, non-invasive means for molecular characterization of cell surface phenotype in vivo, which can in turn guide diagnosis, prognosis, therapy selection, and monitoring of treatment in cancer (Artiko *et al*., 2011).

The clinical value of PET and immunoscintigraphy with ^{131}I or ^{111}In anti- CEA mAb for diagnosis of recurrent colorectal cancer has been confirmed by Ito *et al*., who have concluded that PET/CT reflects more accurately the biological character of tumours, but cannot provide the specificity of immunoscintigraphy that enables us to distinguish patients for antibody-based therapy. The superior value of PET with FDG for detection of distant metastases (liver, bone, and lung) and lymph node involvement has been estimated in comparison to ^{99m}Tc-anti-CEA Fab for detection of recurrence of colorectal carcinoma. Immunoscintigraphy is superior for detection of local recurrent colorectal cancer, whereas PET is better for detection of distal metastases. Radioimmunoguided surgery (RIGS) enables intraoperative detection of small tumour deposits using special gamma probe systems, after intravenous administration of radiopharmaceuticals. Roveda *et al* have performed immunoscintigraphy with ^{131}I or ^{111}In anti-CEA and 19.9 mAb using a gamma probe, and have found it particularly useful for endoscopic study of the pelvis after anterior resection, which is difficult to achieve by other diagnostic procedures. Both immunoscintigraphy and RIGS enable a more accurate diagnosis according to Hladic *et al*. Florio *et al* have found positive intraoperative gamma probe detection, although negative for immunoscintigraphy. RIGS applied in primary colorectal cancer enables the detection of occult lymph node metastases. Imaging methods (CT, US, MRI) have an advantage for detection of liver metastases, whereas immunoscinitgraphy is more specific for the assessment of recurrence of abdominal tumours. Immunoscintigraphy may be applied in patients

with suspected local recurrence and inconclusive results of routine diagnostic workup (Boermen &Oyen, 2011; Heine *et al*., 2011).

Attention has also been given to PET specific tracers. ^{64}Cu anti-GD2 monoclonal antibody (mAb) target antigens overexpressed on neuroblastoma and melanoma. ^{124}I-, ^{64}Cu-, ^{86}Y-Labeled Antibodies are being studied with specific binding to tumour associated antigenic binding sites (such as CEA, PSMA, CD20 and CD22).

Radioimmunotherapy (RIT) is a treatment modality, which uses radiolabelled antibodies in the therapy of cancer. Monoclonal antibodies against a variety of tumour associated antigens have been developed and shown to target tumours with minimal side effects. Numerous radionuclides have been conjugated to antibodies and the radioimmunoconjugates have been shown to be stable in vivo. RIT for relapsed or refractory CD20-positive B-cell NHL means intravenous administration of ^{90}Y-labelled ibritumomab tiuxetan (Zevalin®) (Dillman, 2006). ^{90}Y(III)chloride is produced through decay of the radioactive precursor nuclide 90 Strontium (^{90}Sr). The decay of ^{90}Y is accompanied by the release of beta radiation with a maximum energy of 2.281 MeV (99.98%) into stable 90 Zirconium (^{90}Zr), with a half-life of 64 h (2.7 d). Ibritumomab tiuxetan is a conjugated murine anti-CD20 antibody genetically engineered from Chinese hamster ovary (CHO) line using the MX-DTPA chelating agent. The ibritumomab tiuxetan antibody targets the CD20 antigen, which is expressed on the surface of normal (except for pre-B cells and secretory B cells) and malignant B lymphocytes.

Iodine (^{123}I/^{131}I) labelled Metaiodobenzylguanidine (MIBG)

MIBG is the combination of the benzyl group of bretylium and the guanidine group of guanethidine. It was developed in the early 1980s to visualise tumours of the adrenal medulla. MIBG structurally resembles norepinephrine. It enters neuroendocrine cells by an active uptake mechanism and is stored in the neurosecretory granules. ^{123}I/^{131}I-MIBG is used to image tumours of neuroendocrine origin, particularly those of the sympathoadrenal system (phaeochromocytomas, paragangliomas and neuroblastomas). Subsequent uptake in other neuroendocrine tumours (mostly carcinoids and medullary thyroid carcinoma) has also been reported. ^{123}I/^{131}I-MIBG has also been employed to study disorders of sympathetic innervation, such as that of the heart. MIBG can be labelled with either ^{131}I or ^{123}I. Theoretical considerations and clinical experience indicate that the ^{123}I-labelled agent is to be considered the radiopharmaceutical of choice, at least in children, as it has a more favourable dosimetry and provides better image quality. Nonetheless, ^{131}I-MIBG is widely employed for most routine applications mainly in adult patients because of its lower costs, its ready availability, longer half-life and the possibility of obtaining delayed images. It is an acceptable choice also in children especially when acquisitions are to be repeated over time. Paraganglioma, malignant paraganglioma, ganglioblastoma and neuroblastoma may all be detected with ^{123}I or ^{131}I-MIBG. Thyroid blockade with potassium iodide, lugol's iodine and perchlorate is indicated to limit the dosimetry of free iodine. The clinical indications for includes the localization of adrenal pheochromocytomas and extra-adrenal paragangliomas; the localization of metastatic adrenal medullary cancer secondary to pheochromocytoma; prior to ablation therapy of metastatic adrenal medullary cancer secondary to pheochromocytoma; the evaluation of patients with suspected neuroblastomas; the evaluation of patients with carcinoid and medullary thyroid cancer to determine if ^{131}I-MIBG therapy would be of benefit. (SNM Procedure guidelines; EANM Procedure guidelines)

Gene Expression

Differential expression between disease subgroups has been primarily seen in mitochondrial-, structural-, and transcription-related genes (Sanoudou *et al*., 2004). 9-(4-18F-Fluoro-3-[hydroxymethyl]butyl)guanine (^{18}F-FHBG) is sensitive and specific for imaging the genes, herpes simplex 1 thymidine kinase (HSV1-tk) and its mutant HSV1-sr39tk. These genes have been demonstrated in the livers of hepatocellular cancer patients. Studies are being done on ^{68}Ga-labeled oligonucleotides target activated human K-ras oncogene.

Oncolytic adenoviruses can be engineered for better tumour selectivity, gene delivery and be armed for imaging and concentrating radionuclides into tumours for synergistic oncolysis (Gambhir *et al*., 1999). Temporal and spatial changes in hNIS-expression during therapy were detected with SPECT, have demonstrated feasibility of evaluation of the combination therapy with hNIS-expressing adenoviruses and radioiodide (Fujiwara, 2011).

2.1.5. Iodine Metabolism

Iodine is an essential element which is used in the synthesis of thyroid hormone. Differentiated thyroid cancer (DTC) is among the most curable of cancers yet the presence of incidental thyroid micrometastases (diameter 1 cm or smaller) is 5% to 36% of autopsied adults. The management of DTC is one of the more debated topics in clinical medicine. Significant developments in monitoring and treatment during the past decade have changed many of the traditional approaches to the patient with DTC, some of which remain controversial. The most effective nonsurgical treatment and imaging for differentiated thyroid carcinoma is radioactive iodine (RAI). Radioiodine has 3 main indications in the postoperative management of patients with thyroid cancer: ablation of residual thyroid tissue with ^{131}I, imaging for possible recurrent disease with ^{123}I or ^{131}I, and treatment of residual or recurrent thyroid cancer with ^{131}I. The aim in therapy is to destroy any microscopic foci of disease remaining after the surgery and to destroy any remaining normal thyroid tissue to improve the value of serum Thyroglobulin (Tg) as a tumour marker. If all normal thyroid cells are eliminated by RAI, then any increase in serum Tg in the follow-up of these patients becomes more specific and indicates recurrence of thyroid cancer, and this also increases the specificity of ^{131}I scanning for detection of recurrent or metastatic disease by eliminating uptake by residual normal tissue (LiVolsi, 2011; McHenry & Phitayakorn, 2011). The use of ^{124}I in PET is currently investigational and limited to institutional clinical use.

According to the American Thyroid Association (ATA) revised guidelines (2009) (Cooper *et al*., 2009), risk groups of patients may be classified into low-, intermediate- and high- risk. Low-risk patients have no local or distant metastases; all macroscopic tumour has been resected; there is no tumour invasion of locoregional tissues or structures; the tumour does not have aggressive histology (e.g., tall cell, insular, columnar cell carcinoma) or vascular invasion; and, if ^{131}I is given, there is no ^{131}I uptake outside the thyroid bed on the first post-treatment whole-body RAI scan (RxWBS). Intermediate-risk patients have microscopic invasion of tumour into the perithyroidal soft tissues at initial surgery; presence of cervical lymph node metastases or ^{131}I uptake outside the thyroid bed on the RxWBS done after thyroid remnant ablation; or tumour with aggressive histology or vascular invasion. High-risk patients have macroscopic tumour invasion, incomplete tumour resection, distant metastases, and may present with a thyroglobulinemia out of proportion to what is seen on the RxWBS.

The literature supports the use of ^{18}FDG-PET scanning for indications beyond simple disease localization in Tg-positive, RAI scan–negative patients. Current additional clinical uses of ^{18}FDG-PET

scanning may include initial staging and follow-up of high-risk patients with poorly differentiated thyroid cancers unlikely to concentrate RAI in order to identify sites of disease that may be missed with RAI scanning and conventional imaging (Sandu etal, 2011). It has also been used for the initial staging and follow-up of invasive or metastatic Hurthle cell carcinoma.

2.2. Angiogenesis

Malignant tumours are characterised by the development of chaotic and leaky blood vessels a disturbed microcirculation, low oxygen tension, high interstitial pressure and ultimately insufficient delivery of chemotherapy. Many different features of vascularity permit the distinction between malignant and benign processes, some of which can be interrogated by imaging techniques. Structural and functional characteristics of malignant tumour vasculature include: spatial heterogeneity and chaotic structure; poorly formed, fragile vessels with high permeability to macromolecules; arteriovenous shunting, high vascular tortuosity and vasodilatation; intermittent or unstable blood flow due to transient rises in already raised interstitial pressure; extreme heterogeneity of vascular density with areas of low vascular density mixed with regions of high angiogenic activity. Studies have shown that monitoring tumour angiogenesis has prognostic value.

Angiogenesis is linked to an increased risk of local regional recurrence, distant metastases, and reduced survival in patients with cancers at various organs, including breast, lung, and ovary. A large number of local and circulating angiogenic factors are known to be involved in the angiogenic process, including vascular endothelial growth factor (VEGF), angiopoietins, and basic fibroblast growth factor (bFGF). These molecular processes are being currently studied by many investigators as potential targets for the development of angiogenesis imaging and for the development of novel radiotracers to evaluate both tumour angiogenesis and tumour response to various anti-angiogenesis drugs (Jeswani & Padhani, 2005; Missbach-Guentner *et al*., 2011; Choe & Lee, 2077; Jansen *et al*., 2010; Zhu *et al*., 2010).

2.2.1. Vascular Endothelial Growth Factor and its Receptors (VEGF/VEGFRs)

VEGF is an important angiogenic factor induced by local hypoxia. VEGF induces various functions on endothelial cells by interacting with high affinity tyrosine kinase receptors. VEGF and VEGF receptors (VEGFR) are therefore considered potential targets for angiogenesis imaging. Both SPECT and PET imaging have been performed with radiolabeled anti-VEGF antibodies.

The more rational design is to use radiolabeled VEGF isoforms for SPECT or PET imaging of VEGFR expression. With SPECT imaging, recombinant human VEGF121 was labelled with ^{111}In and ^{99m}Tc through an "Adapter/Docking" strategy. VEGF121 has also been labelled with ^{64}Cu for PET imaging of tumour angiogenesis and VEGFR expression. Micro-PET imaging revealed the dynamic nature of VEGFR expression during tumour progression in that even for the same tumour model, VEGFR expression level can be dramatically different at different stages. The uptake of ^{64}Cu-DOTA-VEGF121 in the tumour peaked when the tumour size was about 100–250 mm^3.

Peptidic VEGFR antagonists can be labelled with short-lived isotopes such as ^{18}F. Labelling has also been reported with ^{188}Re for SPECT imaging of VEGFR in tumour-bearing nude mice. Planar imaging with SPECT demonstrated significant radioactivity accumulation in tumour 1 h after injection of the labelled peptide and disappearance of radioactivity 3 h later, facilitating repetitive imaging with the peptide for therapy response monitoring (Backer & Backer, 2012).

2.2.2 Integrins

Integrins are a family of receptors comprised of a family of heterodimeric glycoproteins, which are involved in the formation of new blood vessels in tumours. Integrins expressed on endothelial cells are related to cell survival and migration during angiogenesis, while integrins expressed on carcinoma cells modulate metastasis by facilitating invasion and movement across the vessels. The integrin member, which binds to arginine-glycine-aspartic acid (RGD)-containing components of the interstitial matrix such as vitronectin, fibronectin and thrombospondin, is expressed in a number of tumour types such as melanoma, late stage glioblastoma, ovarian, breast, and prostate cancer. Integrin ąvß3 promotes angiogenesis and endothelial cell survival and that antagonism of this integrin suppresses angiogenesis by inducing endothelial cell apoptosis in vitro and in vivo. Integrins are ideal pharmacological targets based on both the key role they played in angiogenesis, leukocytes function and tumour development and easy accessibility as cell surface receptors interacting with extracellular ligands.

^{18}F arginine-glycine-aspartic acid (RGD) peptide binds specifically to ąvß3 intergrins expressed at the surface of activated endothelial cells during angiogenesis. The (RGD) cell adhesion motif was discovered in fibronectin by Pierschbacher and Ruoslahti 20 years ago. This integrin is expressed on the luminal surface of neovasculature but is not found on the endothelial surface of mature capillaries. In addition it has been shown to be upregulated in tumour blood vessels that undergo continuous angiogenesis and has been implicated in metastasis. Synthetic RGD peptide antagonists were subsequently shown to inhibit growth of neovasculature and effect tumour regression in animal models, presumably by starving tumours of their blood supply. ^{18}F-Galacto-RGD has been developed for PET imaging of ąvß3 expression of a receptor involved in angiogenesis and metastases. Beer *et al* tested and established the feasibility of using this tracer in eleven patients with Head and neck squamous cell carcinoma (HNSCC). An important application of this new radiotracer would be in monitoring treatment response of anti-angiogenic therapy (Lewis, 2005).

A variety of radiometalated tracers have been developed as well, including peptides labelled with ^{111}In, ^{99m}Tc, ^{64}Cu, ^{90}Y, ^{188}Re, ^{89}Zr and ^{68}Ga. Most of them are based on the cyclic pentapeptide c(RGDfK) or c(RGDyK) and are conjugated via the ã-amino function of a lysine with different chelator systems, like diethylene triamine pentaacetic acid (DTPA), the tetrapeptide sequence H-Asp-Lys-Cys-Lys-OH, 1,4,7,10-tetraazacyclododecane-1,4,7,10-tetraacetic acid (DOTA) and 1,4,7-triazacyclononane-1,4,7-triacetic acid (NOTA). While all these compounds have shown high receptor affinity and selectivity and specific tumour accumulation, the pharmacokinetics of most of them still need to be improved (Shan, 2013; Zhanga *et al*., 2011).

There are several issues and limitations regarding imaging of Integrins. Integrins are not only overexpressed on tumour endothelial cells but also on tumour cells. There is also heterogeneity of integrin expression between different tumours or even within the same tumour itself. In addition, tumour uptake and accumulation of imaging tracers is not only dependent on the receptor expression. Several other factors including vascular density and volume, vascular permeability and interstitial fluid pressure also affect the distribution (Haubner *et al*., 1999).

2.2.3 Matrix metalloproteinases (MMPs)

MMPs are a family of zinc- and calcium-dependent endopeptidases which are responsible for the enzymatic degradation of connective tissue, and thus facilitate endothelial cell migration during angiogenesis. MMPs play an important role in new blood vessel formation. The MMP specific tracers have been la-

belled with several radionuclides such as ^{99m}Tc, ^{111}In and ^{64}Cu and are still currently under investigation. Significant improvements in tumour MMP targeting and in vivo pharmacokinetics are necessary before the use of MMP radiotracer imaging can be translated into clinical application.

2.2.4. Other Angiogenesis Imaging Targets

The angiogenic response is also modulated by the composition of the extracellular matrix (ECM) and intercellular adhesions, because endothelial cells must adhere to one another and to the ECM in order to construct new microvessels. Fibronectin and vitronectin recruited from plasma also play a key role in ECM remodelling during tumour growth and angiogenesis.

Fibronectin is a large glycoprotein and can be found physiologically in plasma and tissues. Extra-domain B of fibronectin (EDB), consisting of 91 amino acids, is not present in the fibronectin molecule under normal conditions, but expressed in the endometrium in the proliferative phase and some vessels of the ovaries. It is an angiogenesis marker in a variety of solid tumours.

A human antibody fragment scFv (L19) was identified and has been shown to efficiently localize on neovasculature in vivo. The L19 small immunoprotein (SIP) was labelled with ^{76}Br and ^{124}I for PET imaging.

Endoglin (CD105) is a cell membrane glycoprotein mainly expressed on endothelial cells and overexpressed on tumour vasculature. ^{111}In-labeled E-selectin antibody was used for imaging of inflamed human synovial vasculature. Other angiogenesis-related biomarkers, such as angiopoietins/Tie receptors, and CD276 are also potential targets for angiogenesis imaging.

2.3. Hypoxia

Increasing tumour size results in a reduced ability of the local vasculature to supply sufficient oxygen to rapidly dividing tumour cells. To identify and to quantify blood flow and tissue perfusion in tumours or to monitor response to chemotherapy later on, ^{15}O-labeled water was one of the first approved radiolabeled tracers in cancer patients (Wilson *et al*., 1992; Tseng *et al*., 2004). In these studies only functional changes due to alterations of volume distribution of radiolabeled water within the tumour tissue could be determined. Resulting hypoxia may inhibit new cell division or lead to cell death may also lead to activation of certain processes that will help cells survive and progress.

Well-oxygenated cells are more sensitive to the cytotoxic effects of ionizing radiation compared with poorly oxygenated cells. Hypoxia in tumour tissue is an important prognostic indicator of response to therapy. 2-Nitroimidazole (azomycin) was developed in the 1950s as an antibiotic targeted against anaerobic germs. It was only in 1979 that Chapman and coworkers proposed nitroimidazoles as markers of hypoxia and as a sensitizing factor for radiation therapy of hypoxic tumours. Hypoxic cell radiosensitizers (possessing a selective toxicity for the radioresistant hypoxic cells) tested in clinical trials included metronidazole, misonidazole, nimorazole, and tirapazamine.

Although SPECT is more commonly used than PET, and, in particular, ^{99m}Tc has a number of practical advantages that include ready availability at low cost, convenient half-life for hypoxia measurements and versatile chemistry as compared with ^{18}F, the superior spatial resolution and more accurate quantitation with PET makes the latter a better candidate for detection of tumoural hypoxia. Of all the PET tracers that are being evaluated as possible markers of tumour hypoxia, only three have been thoroughly evaluated in a clinical situation: ^{18}F-FMISO, ^{18}F-FDG and ^{64}Cu-ATSM (Mees *et al*., 2009; Jordan &Sonveaux, 2012).

2.3.1. Iodine derivatives

^{123}I-IAZA and ^{125}I-IAZA (^{123}I/ ^{125}I-iodoazomycin arabinoside) have been used for studying tumour hypoxia. A study investigating the use of ^{123}I-IAZA in 51 human patients with newly diagnosed malignancies demonstrated hypoxia in small cell lung cancer and squamous cell carcinoma of head and neck but not in malignant gliomas. The study did, however, demonstrate the feasibility of ^{123}I-IAZA imaging in a clinical setting. Stypinski *et al*. reported the clinical pharmacokinetics of IAZA, the radiopharmacokinetics of ^{123}I-IAZA, total radioactivity kinetics and the radiation dosimetry estimates for six healthy volunteers and concluded that all supported its clinical use for imaging tissue hypoxia. Newer agents based on the azomycin-nucleoside structure such as iodoazomycin galactoside (IAZG), iodoazomycin pyranoside (IAZP), IAZGP and iodoazomycin xylopyranoside (IAZXP) have been developed and are being evaluated.

2.3.2. Technetium derivatives

BMS 181321 was the first ^{99m}Tc-labelled 2-nitroimidazole to be widely studied for imaging but was found not optimal for tumour hypoxia imaging because of in vitro and in vivo instabilities and high background levels in normal tissues. The nitro group of 2-nitroimidazole (NIM) enters the tumour cells and is bioreductively activated and fixed in the hypoxia cells. BRU59-21 is a second-generation analogue of BMS 181321 which shows greater stability in vitro and better characteristics. In a study by Zhang *et al*., BRU59-21 and HL91 were compared directly in the same in vitro systems. Both tracers proved suitable for hypoxia imaging. Zhang *et al*. evaluated the efficacy of [^{99m}Tc]butylene amineoxime (^{99m}Tc-HL91) as a non-invasive marker of tumour hypoxia. Yutani *et al*. found that ^{99m}Tc-HL91 accumulated to significantly higher levels in hypoxic tumour areas and that ^{99m}Tc-HL91 uptake was strongly correlated with the expression of GLUT1 in the viable cancer cell area. Clinical studies concerning the clinical evaluation of ^{99m}Tc-HL91 are limited, however those done have demonstrated that ^{99m}Tc-HL91 is a safe radioligand and that metabolic binding in a large fraction but not all of local squamous cell carcinoma in Head and Neck tumour recurrences may be expected. In a study with 32 patients with non-small cell lung cancer, Li *et al*. showed that hypoxia imaging with ^{99m}Tc-HL91 before radiotherapy may predict tumour response and patient survival.

^{99m}Tc-cyclam-2-nitroimidazole (^{99m}Tc-N4-NIM) has recently been developed for tumour hypoxia imaging. Planar imaging studies confirmed that the tumours could be visualized clearly with ^{99m}Tc-N4-NIM in animal models. Efficient synthesis of N4-NIM was achieved. ^{99m}Tc-N4-NIM may be useful in evaluating cancer therapy (Ali *et al*., 2012).

2.3.3. ^{18}F derivatives

In 1984, ^{18}F-Fluoromisonidazole (FMISO) was introduced as a tracer for determining tumour hypoxia. It binds selectively to hypoxic cells. FMISO diffuses into cells, where it is reduced by enzymes. In necrotic cells, there is no reduction; therefore, no retention occurs. In normoxic cells, the FMISO is reoxidized and eventually diffuses out of the metabolic compartment. In hypoxic cells, further reduction of the FMISO results in cell retention. (Lee & Scott, 2007).

Its high lipophilicity, and slow clearance kinetics, necessitates imaging for longer periods of time post injection. It has been used to evaluate high grade gliomas, renal cell carcinoma low grade uptake, non-small cell lung carcinoma low uptake, and is widely used in head and neck tumours. Studies using FMISO have demonstrated variable, but significant levels of hypoxia in several tumour types. In addition,

FMISO PET imaging has been used as a prognostic indicator in several other studies. It has, however, failed to gain wider acceptance for routine clinical application because of a number of limitations such as: slow accumulation in hypoxic tumours; a low target to background ratio due to high non-specific binding resulting from its relatively high lipophilicity; and significant non-oxygen dependent metabolism leading to a considerable amount of radioactive metabolite products. ^{18}F-fluoroerythronitroimidazole (FETNIM), ^{18}F-fluoroetanidazole (FETA), and 1-(5-^{18}F-Fluoro-5-deoxy--D-arabinofuranosyl)-2-nitroimidazole (FAZA) have been developed with more favorable pharmacokinetics.

Several studies have tried to validate ^{18}F-FDG as an alternative marker for hypoxia imaging. The rationale behind this is that ^{18}F-FDG uptake during FDG PET imaging relies largely on the expression of proteins that are under control of HIF-1. As a result, the degree of ^{18}F-FDG uptake by tumours might in-directly reflect the level of hypoxia. This would obviate the need for more specific radiopharmaceuticals for hypoxia imaging. Reports trying to relate ^{18}F-FDG uptake with tumour hypoxia have given inconsistent results.

2.3.4. Other Pet tracers

^{64}Copper-diacetyl-bis-N4-methylthiosemicarbazone ([^{64}Cu]-CuATSM) is a neutral and lipophilic Copper-2-bis (thiosemicarbizone) that has shown rapid diffusion into cells and has been shown in vitro to be highly selective for hypoxic tissue (Kersemans *et al*., 2011).

2.4. Apoptosis

'Programmed cell death' is central to homoeostasis, normal development and physiology in all multicellular organisms. Dysregulation can lead to the destruction of normal tissues in a variety of disorders; too much apoptosis may result from autoimmune and neurodegenerative diseases; too little apoptosis will result in the growth of tumours. The morphologic changes of apoptosis are preceded by an initiation phase triggered by an array of signals, including a lack of needed growth factors, antihormonal therapy, DNA damage, immune reactions, ischemic injury, ionizing radiation, and chemotherapy. The lag time between exposure to the trigger and the development of observable morphologic signs of apoptosis varies greatly, depending on cell type, type of trigger, intensity and duration of exposure, and the local environmental conditions of the cell. Effective therapy of tumours requires the iatrogenic induction of programmed cell death by radiation, chemotherapy, or both.

A non-invasive imaging method to serially detect and monitor this process in cancer patients undergoing conventional radiation and chemotherapy treatments as well as for the development and testing of new drugs would be desirable. Currently we can classify most apoptosis imaging agents being investigated into 4 categories on the basis of the cellular processes they detect: plasma membrane phospholipid asymmetry and phosphatidylserine (PS) exposure; caspase activation; mitochondrial membrane potential collapse. PS exposure has received the most attention as an imaging target in apoptosis for several reasons: The exposure is a near-universal event in apoptosis it occurs within a few hours of the apoptotic stimulus and it presents a very abundant target (millions of binding sites per cell) that is readily accessible on the extracellular face of the plasma membrane. PS exposure may also be increased in non-apoptic cells lines; in mitogen or anti-body stimulated B and T lymphocytes, granulocytes, mast cells. PS exposure is preceded by cell shrinkage and increased lipid mobility which are both inhibited by blockers of volume regulatory K+ and Cl- ion channels. Balsubramian *et al*., found that PS exposure requires the sustained elevation of cytosolic calcium, an event that can be inhibited by Ca^{2+} channel blockers.

Annexin-V

Uncategorized Annexin-V is a protein which binds to PS lipid residues on inner cell membrane. Annexin V also known as annexin A5 has a molecular weight 36,000. It is an endogenous human protein that is widely distributed intracellularly. Very high concentrations in the placenta and lower concentrations in endothelial cells, kidneys, myocardium, skeletal muscle, skin, red cells, platelets, and monocytes. It is the most widely used phosphatidylserine-directed agent. Studies have been done in Head and neck, breast, non-small cell lung carcinoma, melanoma, bladder carcinoma and lymphoma (Schaper &Reutelingsperger, 2013). Its advantages include a very high affinity for apoptotic cells, ready production by recombinant DNA technology, lack of in vivo toxicity of the protein. ^{99m}Tc-HYNIC-Annexin V is available for imaging and has been used to determine the efficacy of chemotherapy in oncology patients stage 3-4 imaging within 24 hours of commencing chemotherapy. ^{18}F Annexin has since been developed and is one potential imaging agent to visualise programmed cell death. ^{124}I Annexin and ^{64}Cu labelled Streptokinase are still under investigation for cancer use (Blackenberg & Norfray, 2011).

3 General Tumour Imaging Radiopharmaceuticals

3.1. Skeletal Scintigraphy

The normal bone undergoes constant remodelling. There is a balance maintained between osteoclastic (resorptive) and osteoblastic activity. In the pathogenesis of bone metastases (Fili *et al*., 2009), several factors are released by tumour cells that stimulate both osteoclast and osteoblast activity. Excessive new bone formation occurs around tumour cell deposits, resulting in low bone strength and potential vertebral collapse. Osteoclastic and osteoblastic activity releases growth factors that stimulate tumour cell growth, perpetuating the cycle of bone resorption and abnormal bone growth (Coxon *et al*., 2004).

Bone metastases are the most common malignant bone tumour (Mundy, 2002). Skeletal involvement occurs in 30%-70% of all cancer patients, with breast cancer being the leading cause for bone metastases in women and prostate cancer in men, followed by lung cancer. Detection of bone metastases is essential for optimal tumour therapy. A malignant lesion may be detected on a bone scan as early as a year prior to being detected on anatomical imaging. It has been estimated that up to 75% reduction in bone density is required to visualize a metastasis on x-ray.

The purpose of imaging is to identify bone metastases as early as possible, to determine the full extent of disease, to evaluate the presence of complications that may accompany malignant bone involvement (including pathologic fractures and spinal cord compression), to monitor response to therapy, and, occasionally, to guide biopsy if histological confirmation is indicated.

3.1.1. Methylene Diphosphonate (MDP)

^{99m}Tc-MDP is the common agent used for bone imaging. It is an organic analogue of pyrophosphate and contains an organic P-C-P bond. The agent affixes to the bone surface by the process of chemisorption attaching to hydroxyapatite crystals in bone and calcium crystals in mitochondria. After administration, it is postulated that ^{99m}Tc-MDP dissociates into its technetium and MDP moieties which are then adsorbed onto the organic and inorganic (hydroxyapatite) phases, respectively. About 40-50% of the compound will be affixed to bone by 3 to 4 hours after injection. The labelling efficiency for ^{99m}Tc-MDP is typically 95%. Excretion is primarily renal. Clinicians have described early detection of renal pathology seen on a

bone scan. By 6 hours, approximately 70% of the administered dose is eliminated. Bone scanning with ^{99m}Tc-MDP detects abnormalities of bone metabolism as early as 24 to 48 hours after the onset of pathology and is nearly always positive by 8 days. Thus, fractures and other manifestations of bone stress can be diagnosed very sensitively by bone scintigraphy. The oncological indications for bone scintigraphy with MDP are for primary tumours (e.g. Ewing's sarcoma, osteosarcoma); staging, evaluation of response to therapy and follow-up of primary bone tumours, secondary tumours (metastases); staging and follow-up of neoplastic diseases, and the distribution of osteoblastic activity prior to radiometabolic therapy (such as ^{89}Sr, ^{153}Sm-EDTMP and ^{186}Re-HEDP). (SNM Procedure guidelines; BNMS Procedure guidelines; EANM Procedure guidelines).

3.1.2. ^{18}F-Fluoride (^{18}F)

^{18}F-Fluoride was introduced as a bone-imaging agent by Blau *et al*. in 1962. The FDA approved the New Drug Application (NDA) for bone imaging to define areas of altered osteogenic activity in 1972. Fluoride ions are chemisorbed onto bone surface by exchanging with hydroxyl (OH) groups in hydroxyapatite ($Ca^{10}(PO_4)^6(OH)^2$) crystal of bone to form flouroapatite. Uptake is related to blood flow and bone remodelling or turnover. The use of ^{18}F in hybrid PET/CT imaging has significantly improved the specificity, because the CT component of the study allows morphologic characterization of the functional lesion and more accurate differentiation between benign lesions and metastases. ^{18}F bone scans may be used to identify skeletal metastases, including localization and determination of the extent of disease. (SNM Procedure guidelines)

3.2. Methoxy-isobutyl-isonitrile (MIBI)

^{99m}Tc labelled MIBI was first described in 1984, by Jones *et al*., as a myocardial perfusion tracer. In 1990, Delmon-Moingeon *et al*., described MIBI as an in vivo tumour imaging agent and was fortuitously observed to show uptake in tumours of the lung, thyroid, brain, lymph node metastasis, bone and in breast cancer. MIBI has found a role in breast scintigraphy in the following indications: detection of breast cancer when mammography is doubtful, inadequate or indeterminate; as a complementary procedure in patients with doubtful microcalcifications or parenchymal distortions; scar tissue in the breast following surgery or biopsy in mammographically dense breast tissue; breasts with implants; identifying multicentric, multifocal or bilateral breast cancer in patients with a diagnosis of breast cancer (Bombardieri *et al*., 2003).

The cellular uptake of MIBI is due to passive influx of the lypophilic cation and is driven by the plasma and mitochondrial membrane potentials generated in living cells. MIBI non-specifically localizes in mitochondria and the cytoplasm in response to elevated membrane potentials across the membrane bilayers of the cell and mitochondria. MIBI has been reported to localize non-specifically in a variety of malignant and non-malignant tumours. Enhanced uptake of ^{99m}Tc MIBI in malignant tumours is thought to reflect the increased numbers of mitochondria in cancer cells. Although the exact uptake mechanisms into the myocardial and tumour cells are not well understood, it is postulated to be related to blood flow, blood residence time, and the cellular uptake due to passive influx of the lipophilic cation, driven by the plasma and mitochondrial membrane potentials generated in living cells. Elevated potentials are directly related to metabolic state. A modulatory factor for MIBI uptake may be associated with the overexpression of P-glycoprotein in tumours, but it remains unknown about the exact underlying mechanism and relationship to MIBI. It has been observed that the lower MIBI uptake in certain histologically confirmed tumours such as bronchioloalveolar carcinoma was related to an overexpression of P-glycoprotein as an

in vivo marker of multidrug resistance. MIBI is physiologically taken up by the salivary glands, thyroid, heart, liver, spleen, and skeletal muscle. There is physiological hepato-biliary and renal clearance. The advantages include a readily available kit, easy to prepare, cost effective for a large patient-base, reasonable radiation dosimetry with good quality images from the 140keV single gamma photon energy of ^{99m}Tc (Moretti *et al*., 2005).

3.3. Gallium 67 Citrate (^{67}Ga)

^{67}Ga has been used for imaging a variety of solid tumours since 1969. ^{67}Ga is cyclotron produced. It has a physical half-life of 78 hours and a biological half-life of 2-3 weeks. After intravenous administration, ^{67}Ga is bound to transferrin in the blood, and distributed to liver, lacrimal glands, salivary glands, and soft tissue tumors. Within the cells of the liver and tumors, gallium is found in lysosomes, and rough endoplasmic reticulum. Within these organelles, ^{67}Ga is bound to a variety of macromolecules, including transferrin, ferritin, and a 45,000 molecular weight glycoprotein. ^{67}Ga imaging of neoplastic disease has shown the greatest utility in imaging lymphomas but it can also be used for other tumours. In addition, ^{67}Ga has been employed to detect chronic infections (such as sarcoidosis), to evaluate interstitial lung disease, and to examine patients with acquired immunodeficiency syndrome (AIDS). Clinical usefulness of ^{67}Ga has been suggested for the study of adults presenting with fever of unknown origin because of the possibility of locating pathological uptake (both malignant and benign). The main indication for ^{67}Ga scintigraphy is lymphoma (Hodgkin's disease, HD, and non-Hodgkin's lymphoma, NHL), for evaluation of response to treatment, assessing tumour viability in the presence of post-therapy residual disease detected by conventional radiological tools such as CT or MRI.

It is a prognostic indicator in the prediction of outcome; evaluation of disease extent. The accuracy of ^{67}Ga scan is not superior to that of CT or MRI in staging lymphomas at presentation; however, it may be useful prior to therapy as a reference for treatment monitoring. ^{67}Ga is more effective in restaging because of the frequent presence of anatomical distortions/alterations following treatment. ^{67}Ga uptake correlates with tumour cell type and proliferation rate. High ^{67}Ga avidity is shown by diffuse large cell lymphomas including diffuse histiocytic lymphoma and poorly differentiated lymphocytic lymphoma. Similar ^{67}Ga avidity is shown by high-grade and intermediate-grade lymphomas including Burkitt's lymphoma. ^{67}Ga avidity in low-grade lymphomas (e.g. well-differentiated lymphocytic lymphoma) seems to be low. For these reasons a gallium scan is necessary before therapy in untreated patients in order to evaluate whether lymphoma is gallium avid or not. If the ^{67}Ga scan is negative, it should not be repeated. Although the following non-lymphomatous tumours show ^{67}Ga avidity, the usefulness of ^{67}Ga scanning in these patients has not been clearly demonstrated. ^{67}Ga scanning can be employed to image lung cancer, head and neck tumours, hepatocellular carcinoma, germ cell tumours, neuroblastoma, sarcoma, multiple myeloma, and melanoma. ^{67}Ga is indicated for the examination of adults presenting with fever of unknown origin because of the possibility to locate pathological uptake (both malignant and benign) (SNM Procedure guidelines; EANM Procedure guidelines).

3.4. Thallium 201 (^{201}Tl)

^{201}Tl has been utilized in the study of a variety of tumours since 1976. ^{201}Tl is cyclotron produced. It has a physical half-life of 73 hours and a biological half-life of 11 days. It decays by electron capture and emits photons with an energy range of 68- 80keV. ^{201}Tl accumulates mainly within viable tumour tissue, less within connective tissue which contains inflammatory cells, and its accumulation is barely detectable in necrotic tissue. Cellular uptake of ^{201}Tl is not affected by steroids, chemotherapy, or radiation therapy.

Localization of ^{201}Tl within tumours is likely multifactoral and in part related to blood flow, tumour viability, the sodium-potassium adenosine-tri-phosphatase (ATP) system, the non-energy dependent co-transport system, the calcium ion channel system, vascular immaturity with leakage, and increased cell membrane permeability. Radiation therapy and chemotherapy do not appear to immediately inhibit ^{201}Tl uptake as they do ^{67}Ga accumulation. Imaging has been reported in Head and neck carcinomas, breast carcinoma, bone malignancies, lymphoma and soft tissue sarcomas. A baseline pretreatment determination of ^{201}Tl avidity in the tumour is crucial to its efficacy in therapeutic response assessment. The optimal time for ^{201}Tl tumour imaging is 20 to 60 minutes post injection. Delayed images at 3 hours are recommended when imaging lymphoma because of an improved lesion to background ratio on the later images. Spot views of the lesion should be 5 minute preset timed images using a high resolution collimator. The normal distribution of ^{201}Tl within the body is choroid plexus of the lateral ventricles, lacrimal glands, salivary glands, thyroid, myocardium, liver, spleen, splanchnic areas, kidneys, and testes. There is also uniform muscle uptake. Bone marrow activity should not be seen, and if noted indicates marrow hyperplasia. There is little uptake in healing surgical wounds. The kidneys are the critical organ. Unfortunately, ^{201}Tl does not demonstrate 100% specificity for tumours and false-positive uptake has been seen in histiocytosis X, benign bone tumours, stress fractures, and inflammation (Sugawara *et al*., 2005).

3.5. ^{99m}Tc-labelled HMPAO

^{99m}Tc hexamethyl propylamine oxime (99mTc-HMPAO, Ceretec, Amersham Ltd., U.K.), also known as ^{99m}Tc-exametazime, is a lipid soluble macrocyclic amine. It is a brain perfusion imaging agent. Brain uptake of the radiotracer is rapid and reaches its maximum within 10 minutes post-injection time. The distribution of the radiotracer remains constant for many hours post-injection. Once it crosses the blood brain barrier, ^{99m}Tc-HMPAO is converted into a hydrophilic compound in the presence of intracellular glutathione and is trapped, with slow blood clearance. Both primary and metastatic brain tumour lesions present on SPECT brain perfusion imaging as localized defects that correspond to the mass lesions. This technique alone is of limited value in the primary diagnosis or evaluation of intracranial mass lesions. In conjunction with ^{201}Tl, however, SPECT brain perfusion imaging may be valuable in distinguishing between radiation necrosis and tumour recurrence in patients with malignant gliomas treated with high dose radiation. The study may also localize suspected recurrences for biopsy (Groshar *et al*., 1993).

	Pathway	Tracers	Clinical/Investigated Applications
Metabolic	Glucose metabolism	FDG	Staging on presentation in non-small-cell lung cancer, T3 oesophageal cancer, Hodgkin's disease, non-Hodgkin's lymphoma, locally advanced cervical cancer, ENT tumours with risk factors and locally advanced breast cancer. Differentiation of benign and malignant lesions (such as a solitary lung nodule, especially in case of discrepant clinical and radiological estimates of the likelihood of cancer). Evaluation of response to therapy in malignant lymphoma and GIST. Restaging in the event of potentially curable relapse for FDG avid tumours. Diagnosis of unknown primary malignancy, Establishing and localizing disease sites as a cause for elevated serum markers (this includes colorectal, thy-

			roid, ovarian, cervix, melanoma, breast and germ-cell tumours). Image guided biopsy Radiotherapy planning.
	Lipid and fat	Choline	Evaluating prostate carcinoma, high grade gliomas, anaplastic astrocytomas and primary hepatocellular cancer
		Acetate	Evaluating Prostate carcinoma
	Proliferation (DNA metabolism)	Thymidine analogues	Primary lung carcinoma, high grade gliomas, lymphoma (aggressive cell type), breast cancer, (early assessment response to chemotherapy), colorectal carcinoma, head and neck carcinoma, melanoma, soft tissue sarcoma of extremities.
	Amino Acids and Protein metabolism	Radiolabelled amino Acids	Low grade glioblastoma, glioblastoma (mild uptake), meningioma (high uptake)
		Radiolabelled peptides	
		SSRI	Identify/localize Neuroendocrine malignancies, Evaluating disease extent, monitoring effects of therapy, selecting patients for therapy, and prognostic indicator.
		Dopamine	Evaluate melanomas, neuroendocrine tumours, medullary thyroid carcinoma, pheocromocytomas, gastrointesitinal carcinoid tumours, brain tumours; mostly metastatic tumours and malignant gliomas superior in evaluating recurrent low-grade and high-grade gliomas.
		Tumour specific Receptors	Mostly evaluating and monitoring treatment response in Breast and Prostate carcinomas
		Monoclonal Antibodies	Detection of occult disease, in the management of patients with potentially resectable disease, and for the evaluation of lesion recurrence and therapeutic response mostly Prostate and Colorectal carcinoma,
		Guanidine analogue (MIBG)	Tumours of neuroendocrine origin, particularly those of the sympathoadrenal system (phaeochromocytomas, paragangliomas and neuroblastomas).
		Gene expression	Hepatocellular carcinoma
	Iodine metabolism	Iodine	Differentiated Thyroid carcinoma
Angiogenesis		VEGF/VEGFRs Integrins MMPs	Melanoma, late stage glioblastoma, ovarian, breast, and prostate cancer
Hypoxia		Nitromidazole derivatives	Head and neck, high grade gliomas, and lung carcinoma
Apoptosis		Annexin-V	Head and neck, breast, non-small cell lung carcinoma, melanoma, bladder carcinoma and lymphoma
General tumour imaging radiopharmaceuticals	Skeletal	Methylene Diphosphonate	Evaluating primary tumours (e.g. Ewing's sarcoma, osteosarcoma); staging, evaluation of response to therapy and follow-up of primary bone tumours, secondary tumours (metastases); staging and follow-up of neoplastic diseases, and the distribution of osteoblastic activity prior to radiometabolic therapy.

		Flouride	Identify skeletal metastases, including localization and determination of the extent of disease
	Mitochondrial activity	MIBI	lung, thyroid, brain, lymph node metastasis, bone and in breast carcinoma
	Transferrin receptor mechanism	Gallium 67 citrate	Mostly lymphoma (Hodgkin's disease, HD, and non-Hodgkin's lymphoma, NHL), for evaluation of response to treatment, assessing tumour viability in the presence of post-therapy residual disease detected by conventional radiological tools such as CT or MRI
	Na-K adenosine-triphosphatase (ATP) system	Thallium 201	Head and neck, breast, bone, lymphoma and soft tissue sarcomas
	Lipophilic brain perfusion agent converted by glutathione	HMPAO	Used in conjunction with ^{201}Tl and other brain tumour agents to localize recurrences for biopsy.

Table 4: Summary list of tracers and clinical indications.

4 Theranostics

Theranostics is a combination of two words, therapy and diagnosis. The term theranostics epitomizes the inseparability of diagnosis and therapy, the pillars of medicine. Under ideal circumstances the diagnostician uses an agent that is highly specific for diagnosing the pathology. The therapist then utilizes a variation of the same agent so that the same disorder which the physician is dealing with and from which the patient is suffering is treated. The goal in management is maximum efficiency and minimum complications.

In Nuclear Medicine, this refers to the use of molecular targeting vectors (e.g. peptides). These vectors are labelled with diagnostic radionuclides [e.g. positron or gamma emitters], or with therapeutic radionuclides (e.g. beta or alpha emitters, Table 5) for diagnosis and therapy of a particular disease which is targeted specifically by the vector at its molecular level. Therefore molecular imaging and diagnosis of the disease can be effectively followed by personalized treatment utilizing the same molecular imaging vectors (Figure 1 and Figure 2 *adapted from General introduction to therapeutic nuclear medicine by C.A. Hoefnagel*). Table 5 represents a list of selected radionuclides currently being used for therapy and their characteristics which make them each unique for their purpose. The idea of tailored management and individualizing therapy has now been achieved and has opened a door for new and greater opportunities ahead (Lee & Li, 2011; Freeman & Blaufox, 2012; Baum & Kulkarni, 2012; Goldenberg *et al*., 2012).

Acknowledgements

Dr Masha Maharaj: Thank You to the Lord Almighty who kept me focused on the work ahead and sustained me. I am truly grateful to my parents and my family for their support and encouragement in pursuit of excellence. A special thank you to my dear brother, Dr Shane Maharaj, who has through Christ Jesus conquered cancer and has inspired me in this field of Medicine. Thank you to my mentor and friend Prof Ajit Padhy. Finally, I thank the dedicated staff at Polokwane Provincial Hospital, Dr AG Frankl, Mr X Mqhayisa, Mrs F Rasool, Mr J Manamela and Mrs Kgakgudi for their support. Dr Nisaar Korowlay: I would like to thank my son Mohammed Baaqir for his love and support.

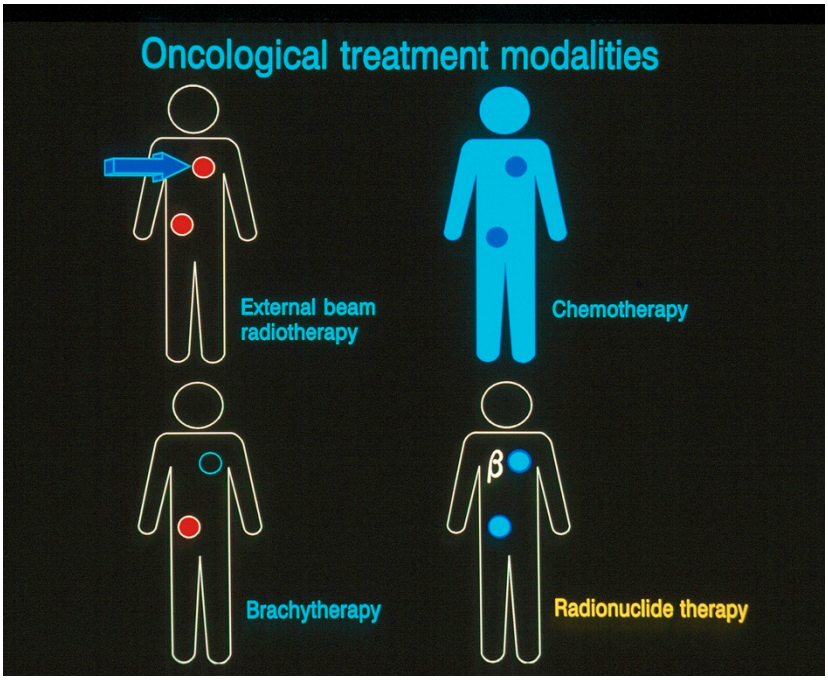

Figure 1: Oncological treatment modalities.

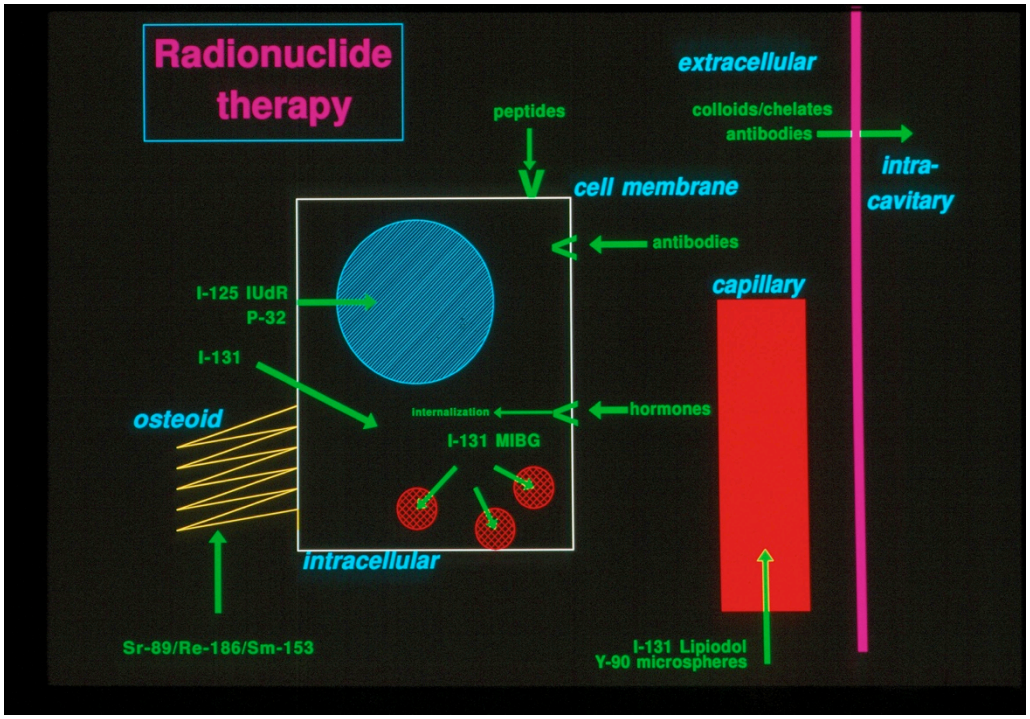

Figure 2: Multiple targeting vectors (Hoefnagel, 1998).

Radionuclide	Halflife	Emission	Maximum range in tissue
Bromiun-80m (80m Br)	4.42 h	Auger electrons	<10 nm
Iodine-125 (125I)	60 d	Auger electrons	10 nm
Astatine-211 (211At)	7.2 h	α	65 nm
Erbium-169 (169Er)	9.5 d	β-	1 mm
Lutetium-177 (177Lu)	6.71 d	β-/γ	2.1 mm
Copper-67 (67Cu)	2.58 d	β-/γ	2.2 mm
Iodine-131 (131I)	8.04 d	β-/γ	2.4 mm
Samarium-153 (153Sm)	1.95 d	β-/γ	3.0 mm
Gold-198 (198Au)	2.7 d	β-/γ	4.4 mm
Rhenium-186 (186Re)	3.77 d	β-/γ	5.0 mm
Dysprosium-165 (165Dy)	2.33 h	β-/γ	6.4 mm
Strontium-89 (89Sr)	50.5 d	β-	8.0 mm
Phosphorus-32 (32P)	14.3 d	β-	8.7mm
Yttrium-90 (90Y)	2.67 d	β-	12mm

Table 5 Selected radionuclides used for therapy and their characteristics

Conflict of interest

None.

References

Ali MS, Kong F, Rollo A, Mendez R. (2012). Development of 99mTc-N4-NIM for Molecular Imaging of Tumor Hy-poxia. Journal of Biomedicine and Biotechnology. Article ID 828139, 1-9

Arens J, Troost E. (2011). FDG-PET/CT in radiation treatment planning of head and neck squamous cell carcinoma. Q J Nuc Med Mol Imaging. 55: 521-528

Artiko V, MarkoviĆ A, ŠobiĆ-ŠaranoviĆ D, PetroviĆ M. (2011). Monoclonal immunoscintigraphy for detection of metastasis and recurrence of colorectal cancer. World J Gastroenterol. 17(19): 2424-2430

Backer MV, Backer JM. (2012). Imaging Key Biomarkers of Tumor Angiogenesis. Theranostics. 2(5):502-515

Badgaiyan R. (2011). Neurotransmitter Imaging: Basic Concepts and Future Perspectives. Current Medical Imaging Reviews. 7, 98-103

Bading J, Shields A. (2008). Imaging of Cell Proliferation: Status and Prospects. J Nucl Med. 49:64S–80S

Baum R, Kulkarni HR. (2012). THERANOSTICS: From Molecular Imaging Using Ga-68 Labelled Tracers and PET/CT to Personalized Radionuclide Therapy – The Bad Berka Experience. Theranostics. 2(5):437-447

Baum RP, Niesen A, Leonhardi J, et al. (2005). Receptor PET/CT imaging of neuroendocrine tumours using the Ga-68 labelled, high affinity somatostatin analogue DOTA-1-Nal3-octreotide (DOTA-NOC): clinical results in 327 patients. Eur J Nucl Med Mol Imaging. 32:S54 (abstr)

Baum RP, Prasad V, Hommann M, Horsch D. (2008). Receptor PET/CTimaging of neuroendocrine tumours. Recent Results. Cancer Res 170:225–42.

Beirsack H, Briele B, Hotze A, Oehr P. (1992). The role of Nuclear Medicine in Oncology. Annals of Nuclear Medicine. Vol 6 (3): 131-136

Blankenberg F, Norfray F. (2011). Multimodality Molecular Imaging of Apoptosis in Oncology. AJR. 197:308–317

Boerman O, Oyen J. (2011). Immuno-PET of Cancer: A Revival of Antibody Imaging. J Nucl Med. Vol. 52 • No. 8: 1171-1172

Bombardieri E, Aktolun C, Baum RP, Bishof-Delaloye A, Buscombe J, et al. (2003). Breast scintigraphy procedure guidelines for tumour imaging. EANM Guidelines.

Chen K, Chen X. (2011). Positron Emission Tomography Imaging of Cancer Biology: Current Status and Future Prospects. Semin Oncol. 38(1): 70–86

Choe Y, Lee KH. (2007). Targeted In Vivo Imaging of Angiogenesis: Present Status and Perspectives. Current Pharmaceutical Design. 13, 17-31

Cooper DS, Doherty GM, Haugen BR, Kloos RT, Lee Sl. et al. (2009). Revised American Thyroid Association Management Guidelines for Patients with Thyroid Nodules and Differentiated Thyroid Cancer. THYROID. Volume 19, Number 11

Coxon JP, Oades GM, Colston KW, Kirby RS. (2004). Advances in the use of bisphosphonates in the prostate cancer setting. Prostate Cancer Prostatic Dis. 7(2):99-104.

Debergh I, Vanhove C, Ceelen W. (2012). Innovation in Cancer Imaging. Eur Surg Res. 48:121–130

Dillman RO. (2006). Radioimmunotherapy of B-cell lymphoma with radiolabelled anti-CD20 monoclonal antibodies. Clin Exp Med. 6:1–12

Fahey H, Treves T, Adelstein J. (2011). Minimizing and Communicating Radiation Risk in Pediatric Nuclear Medicine. J Nucl Med. 52:1240–1251

Fili S, Karalaki M, Schaller B. (2009). Mechanism of bone metastasis: the role of osteoprotegerin and of the host-tissue microenvironment-related survival factors. Cancer Lett. 283(1):10-9

Fouge C, Suchorska B, Bartenstein P, Kreth F. (2011). Molecular imaging of gliomas with PET: Opportunities and limitations. Neuro-Oncology. 13(8):806–819

Freeman L, & Blaufox D. (2012). Theranostics. J.Semnuclmed. Vol 42(3): 145-146

Freeman L, Blaufox D. (2012). PET/CT in Radiation Oncology. J.Semnuclmed. Vol 42(5): 281-282

Freeman LM, Blaufox D. (2013). Letter from the Editors: Low-Sensitivity FDG-PET Studies. J. Semnuclmed. Vol 42 (5): 219-220

Fujiwara T. (2011). A Novel Molecular Therapy Using Bioengineered Adenovirus for Human Gastrointestinal Cancer. Acta med Okayama. Vol 65. 3. 151-162

Gambhir SS, Barrio JR, Phelps ME, Lyer M. (1999). Imaging adenoviral-directed reporter gene expression in living animals with positron emission tomography. Proc. Natl. Acad. Sci. Vol. 96, pp. 2333–2338

Gambhir SS, Czernin J, Schwimmer J, Silverman D, Coleman R, et al. (2001). A Tabulated Summary of the FDG PET Literature. J Nucl Med 42:1S–93S

Gnanasegaran G, Kapse N, Buscombe J. (2005). Recent Trends in Radionuclide Imaging and Targeted Radionuclide Therapy of Neuroendocrine Tumours. IJNM. 20(3): 55-66

Goldenberg M, Chang CH, Rossi E, McBride W. (2012). Pretargeted Molecular Imaging and Radioimmunotherapy. Theranostics. 2(5):523-540

Groshar D, McEwan A, Parliament M, Urtasun R, Golberg L, et al. (1993). Imaging Tumor Hypoxia and Tumor Perfusion. J Nucl Med. 34:885-888

Gunn R, Gunn S, Turkheimer F, AstonJ, Cunningham V. (2002). Positron Emission Tomography Compartmental Models: A Basis Pursuit Strategy for Kinetic Modelling. J Cereb Blood Flow Metab. Dec;22(12):1425-39

Haberkorn U, Markert A, Eisenhut M, Mier W, Altmann A. (2011). Development of molecular techniques for imaging and treatment of tumours. Q J Nuc Med Mol Imaging. 55: 655-670

Hanahan D, Weinberg RA. (2011). Hallmarks of cancer: the next generation. Cell. 144(5):646-74

Haubner R, Wester H, Reuning U, Senekowitsch-Schmidtke R. (1999). Radiolabeled $\alpha V \beta 3$Integrin Antagonists: A New Class of Tracers for Tumor Targeting. J NucI Med. 40:1061-1071

Heine M, Nollau P, Masslo C, & Nielsen P. (2011). Investigations on the Usefulness of CEACAMs as Potential Imaging Targets for Molecular Imaging Purposes. PLoS ONE. Vol 6 (12): e28030

Hicks, R, Hofman, M. (2012). Is there still a role for SPECT-CT in oncology in the PET-CT era? Nature Reviews Clinical Oncology. 9, 712-720

Hoefnagel C. (1998). Radionuclide cancer therapy. Annals of Nuclear Medicine. Vol 12, No. 2, 91-70

Jadvar H. (2011). Prostate Cancer: PET with 18F-FDG, 18F- or 11C-Acetate, and 18F- or 11C-Choline. J Nucl Med. 52:81–89

Jaffer F & Weissleder R. (2005). Molecular Imaging in the Clinical Arena. JAMA. 293(7):855-862

Jansen J, Koutcher J, Shukla-Dave A. (2010). Non-invasive imaging of angiogenesis in head and neck squamous cell carcinoma. Angiogenesis. 13(2): 149–160

Jeswani_T, Padhani.AR. (2005). Imaging tumour angiogenesis. Cancer Imaging. 5, 131–138

Jora C, Mattakarottuc J, Aniruddha PG, & Mudalsha R. (2011). Comparative evaluation of 18F-FDOPA, 13N-AMMONIA, 18F-FDG PET/CT and MRI in primary brain tumours - A pilot study. Indian J Nucl Med. Apr-Jun; 26(2): 78–81

Jordan B, Sonveaux P. (2012). Targeting tumour perfusion and oxygenation to improve the outcome of anticancer therapy. Frontiers in Pharmacology: Pharmacology of Anti-Cancer Drugs. Vol 3; Article 94: 1-15

Joseph AT. (2004). Understanding the Standardized Uptake Value, Its Methods, and Implications for Usage. J Nucl Med. vol. 45 no. 9 1431-1434

Kam B, Teunissen JM, Krenning EP, De Herder W. (2012). Lutetium-labelled peptides for therapy of neuroendocrine tumours. Eur J Nucl Med Mol Imaging. Vol 39 (Suppl 1):S103–S112

Kanwar JR, Roy K, Kanwar RK. (2011). Chimeric aptamers in cancer cell-targeted drug delivery. Critical Reviews in Biochemistry and Molecular Biology. 46(6): 459–477

KaraosmanoĞlu A, Blake M. (2012). Applications of PET-CT in patients with esophageal cancer. Diagn Interv Radiol. 18:171–182

Kersemans V, Cornelissen B, Hueting R, Tredwell M, Hussien K, et al. (2011). Hypoxia Imaging Using PET and SPECT: The Effects of Anesthetic and Carrier Gas on [64Cu]-ATSM, [99mTc]-HL91 and [18F]-FMISO Tumor Hypoxia Accumulation. PLoS ONE. 6(11): e25911

Khan MU, Khan S, El-Refaie S, Win Z, Rubello D, Al-Nahhas A. (2009). Clinical indications for Gallium-68 positron emission tomography imaging. EJSO 35 561-567

Kumar R. (2008). Oncological PET tracers beyond [18F] FDG and the novel quatitative approaches in PET imaging. Q J Nuc Med Mol Imaging. 52: 50-65

Kyoichi K, Masahiro E, Masato A, Kazuo N, Yasuhisa O, et al. (2010). Biologic Correlation of 2-[18F]-Fluoro-2-Deoxy-D-Glucose uptake on Positron Emission Tomography in Thymic Epithelial Tumors. J Clin Oncol. 28:3746-3753

Kyoichi K, Noboru O, Noriaki S, Tamotsu I, Shimizu K, et al. (2011).A systemic review of PET and biology in lung cancer. Am J Transl Res. 3(4):383-391

Kyoichi K, Takehiro O, Yasuhisa O, Toshiaki T, Haruyasu M, et al. (2011). Correlation Between 18F-FDG Uptake on PET and Molecular Biology in Metastatic Pulmonary Tumors. J Nucl Med 52:705–711

Larson S. (1978). Mechanisms of localization of gallium-67 in tumors. Seminars in Nuclear Medicine. Vol.8. Issue 3, 193–203

Laverman P, Sosabowski J, Boerman O, Oyen W. (2012). Radiolabelled peptides for oncological diagnosis. Eur J Nucl Med Mol Imaging. 39 (Suppl 1):S78–S92

Lee D, Li KP. (2011). Molecular Theranostics: A Primer for the Imaging Professional. AJR. . 197:318–324

Lee SZ, Scott A. (2007). Hypoxia Positron Emission Tomography Imaging With 18F-Fluoromisonidazole. Semin Nucl Med 37:451-461

Leitha T. (2009). Nuclear medicine: proof of principle for targeted drugs in diagnosis and therapy. Curr Pharm Des. 15(2):173-87

Lewis MR. (2005). Radiolabeled RGD Peptides Move Beyond Cancer: PET Imaging of Delayed-Type Hypersensitivity Reaction. J NucI Med. Vol. 46 (1): 2-4

LiVolsi V. (2011). Papillary thyroid carcinoma: an update. Modern Pathology. Vol 24, S1–S9

Maecke HR., Hofmann M; Haberkorn U. (2005). 68Ga-Labeled Peptides in Tumor Imaging. J Nucl Med. 46:172S–178S

Mankoff D, Link JM, Linden HM, Sundararajan L. (2008). Tumor Receptor Imaging. J Nucl Med. 49:149S–163S

Mariani, G, Flotats, A, Israel, O, Kim, E.E, Kuwert, T. (2008). Clinical Applications of SPECT/CT: New Hybrid Nuclear Medicine Imaging System. IAEA Doc.

Marnett LJ. (2012). Inflammation and Cancer: Chemical Approaches to Mechanisms, Imaging, and Treatment. J. Org. Chem. 77, 5224−5238

McHenry CR, Phitayakorn R. (2011). Follicular Adenoma and Carcinoma of the Thyroid Gland. The Oncologist 16:585–593

Mees G, Dierckx R, Vangestel C, Van de Wiele C. (2009). Molecular imaging of hypoxia with radiolabelled agents. Eur J Nucl Med Mol Imaging. Vol 36:1674–1686

Missbach-Guentner J, Hunia J, Alves F. (2011). Tumor blood vessel visualization. Int. J. Dev. Biol. 55: 535-546

Moretti J, Hauet N, Caglar M, Rebillard O, Burak Z. (2005). To use MIBI or not to use MIBI? That is the question when assessing tumour cells. Eur J Nucl Med Mol Imaging. 32:836–842

Multhoff &, Radons J. (2012). Radiation, inflammation, and immune responses in cancer. Frontiers in Oncology: Molecular and Cellular Oncology. Vol 2 (58): 1-18

Mundy GR.(2002). Metastasis to bone: causes, consequences and therapeutic opportunities. Nature reviews: Cancer. Vol 2: 284-293

Ni1 X, Castanares M, Mukherjee A, Lupold S. (2011). Nucleic acid aptamers: clinical applications and promising new horizons. Curr Med Chem. 18(27): 4206–4214

Oikonen V. (2005). NET and [18F]FDOPA PET: Literature review. Turku PET Centre Modelling report. TPCMOD0018

Park JW, Cho CH, Jeong DS, Chae HD. (2011). Role of 18F-fluoro-2-deoxyglucose Positron Emission Tomography in Gastric GIST: Predicting Malignant Potential Pre-operatively. J Gastric Cancer. 11(3):173-179

Picchio M, and Castellucci P. (2012). Clinical Indications of 11C-Choline PET/CT in Prostate Cancer Patients with Biochemical Relapse. Theranostics. 2(3): 313-317

Plotnik D, Emerick L, Krohn K, Unadkat J, L Swartz. (2010). Different Modes of Transport for 3H-Thymidine, 3H-FLT, and 3H-FMAU in Proliferating and Nonproliferating Human Tumor Cells. J Nucl Med. 51:1464–1471

Poeppel TD, Krause BJ, Heusner TA, Boy C, Bockisch A, et al. (2009). PET/CT for the staging and follow-up of patients with malignancies. Eur J Radiol. 70(3):382-392

Ponde DE, Dence CS, Oyama N, Kim J. (2007). 18F-Fluoroacetate: A Potential Acetate Analog for Prostate Tumor Imaging - In Vivo Evaluation of 18F-Fluoroacetate Versus 11C-Acetate J Nucl Med. 48:420–428

Procedure guidelines: British Nuclear Medicine Society (BNMS). http://www.bnms.org.uk

Procedure guidelines: European association of Nuclear Medicine (EANM). http://www.eanm.org

Procedure Guidelines. Society of Nuclear Medicine (SNM). http://interactive.snm.org/index

Ray P. (2011). Multimodality molecular imaging of disease progression in living subjects. J. Biosci. 36(3): 499–504

Roberge D, Vakilian S, Alabed YZ, Turcotte RE, Freeman CR, et al. (2012). FDG PET/CT in Initial Staging of Adult Soft-Tissue Sarcoma. Sarcoma, vol. Article ID 960194, 1-7

Rufini V, Calcagni ML, Baum RP. (2006). Imaging of Neuroendocrine Tumors. Semin Nucl Med. 36:228-247

Salskov A, Tammisetti VS, Grierson J, Vesselle H. (2007). FLT: Measuring Tumor Cell Proliferation In Vivo With Positron Emission Tomography and 3=-Deoxy-3=-[18F]Fluorothymidine. Semin Nucl Med. 37:429-439

Sandu N, Pöpperl G, Toubert E, Arasho B, Spiriev T, et al. (2011). Molecular imaging of potential bone metastasis from differentiated thyroid cancer: a case report. Journal of Medical Case Reports. Vol 5:522

Sanoudou D, Frieden LA, Haslett JN, Kho AT, Greenberg SA, et al. (2004). Molecular classification of nemaline myopathies: "nontyping" specimens exhibit unique patterns of gene expression. Neurobiol Dis. Apr;15(3):590-600

Satoru S, Etsuro H, Tatsuya H, Akio N, Yuji N, et al. (2009). P-glycoprotein expression affects 18F-fluorodeoxyglucose accumulation in hepatocellular carcinoma in vivo and in vitro. Int J Oncol. 34(5):1303-12

Schaper F and Reutelingsperger C. (2013). 99mTc-HYNIC-Annexin A5 in Oncology: Evaluating Efficacy of Anti-Cancer Therapies. Cancers 5, 550-568

Schlyer D. (2004). PET tracers and radiochemistry. Ann Acad Med Singapore. 33: 146-154

Seibyl J, Chen W, Silverman DHS. (2007). 3,4-Dihydroxy-6-[18F]-Fluoro-L-Phenylalanine Positron Emission Tomography in Patients With Central Motor Disorders and in Evaluation of Brain and Other Tumors. Semin Nucl Med. 37:440-450

Shan L. (2013). 111In-Labeled multifunctional single-attachment-point reagent-c [RGDfK]: [111In-MSAP-RGD]. MICAD. PMID: 22934321. [Pubmed]

Shankar V. (2007). 18F-Labeled Positron Emission Tomographic Radiopharmaceuticals in Oncology: An Overview of Radiochemistry and Mechanisms of Tumor Localization. Semin Nucl Med. 37:400-419

Sugawara Y, Kikuchi T, Kajihara M, Semba T, Ochi T, et al. (2005). Thallium-201 scintigraphy in bone and soft-tissue tumors: a comparison of dynamic, early and delayed scans. Annals of Nuclear Medicine Vol. 19, No. 6, 461–468,

Sullivan DC, Gatsonis C. (2011). Response to Treatment Series: Part 1 and Introduction, Measuring Tumor Response—Challenges in the Era of Molecular Medicine. AJR. 197:15–17

Tinsu P and Osama M. (2008). PET/CT in radiation oncology. Med. Phys. 35, 4955

Turaga K, Kvols LK. (2011). Recent Progress in the Understanding, Diagnosis, and Treatment of Gastroenteropancreatic Neuroendocrine Tumors. CA Cancer J Clin. 61:113–132

Valotassiou V, Leondi A, Angelidis G, & Psimadas D. (2012). SPECT and PET Imaging of Meningiomas. The Scientific World Journal. Article ID 412580, 1-11

Weissleder R. (2006). Molecular Imaging in Cancer. Science. Vol 312: 1168-1171

Wiyaporn K, Tocharoenchai C, Pusuwan P, Ekjeen T, Leaungwutiwong S, et al. (2010). Factors Affecting Standardized Uptake Value (SUV) of Positron Emission Tomography (PET) Imaging with 18F-FDG. J Med Assoc Thai. 93 (1): 108-14

Zanoni L, Cerci J, Fonti S. (2011). The use of PET/CT to evaluate response to therapy in Lymphoma. Q J Nucl Med Mol Imaging. 55: 633-647

Zhanga Y, Hongb H, Cai W. (2011). PET Tracers Based on Zirconium-89. Curr Radiopharm. 4(2): 131–139

Zhu L, Niu G, Fang X, Chen X. (2010). Preclinical Molecular Imaging of Tumor Angiogenesis. Q J Nucl Med Mol Imaging. 54(3): 291–308

Ziegler, SI. (2005). Positron Emission Tomography: Principles, Technology, and Recent Developments. Nuclear Physics A 752 679c–687c